

**Master's Thesis in Biology (60 ECTS)**  
**Field of Study: Marine Ecology**

**Use of bubble flotation to improve copepod fisheries:  
Laboratory studies on the physical and behavioural interactions  
of *Calanus finmarchicus* and air bubbles**



**Henrik Jeuthe**

**Department of Aquatic BioSciences  
Norwegian College of Fishery Science  
University of Tromsø  
November 2008**





## ***Abstract***

The current study presents a novel approach to zooplankton harvest in the ocean, where copepods are lifted through the water column and concentrate them at the ocean surface. There they are harvested with a surface skimmer or shallow trawl. The method can potentially reduce fuel costs and unwanted by-catch compared to a conventional plankton trawl.

The optimal bubble size for attachment to *Calanus finmarchicus* was determined to 125-225  $\mu\text{m}$ . Attachment was found on 331 of 604 studied copepods (55%), and the majority (88%) had an attached air volume equal to a 50-300  $\mu\text{m}$  bubble. The attachment ratio has been estimated to 20% for 275-400  $\mu\text{m}$  bubbles, i.e. 20% collisions resulted in attachment (N=40). Copepod behaviour, i.e. escape jumping, is the major cause for detachment. Female *C. finmarchicus* are very resilient jumpers, performing on average 95 jumps, during 2 minutes, before becoming passive. Males are significantly less active.

Bubble driven upwelling contributed more than attachment to lifting copepods through the water column. An attached 500  $\mu\text{m}$  bubble gives the copepod an estimated rise velocity of 4 cm/s, while upwelling velocities ( $V_{\text{up}}$ ) of up to 35 cm/s were created in bubble plumes, 30 cm above the bubbler. The relation between air flow (Q) and created upwelling flow was determined to  $V_{\text{up}} \sim Q^{0.23}$  for small bubbles (mean size  $\sim 150 \mu\text{m}$ ) and  $V_{\text{up}} \sim Q^{0.40}$  for large bubbles (mean size  $\sim 1500 \mu\text{m}$ ).

For flotation to be used successfully in a zooplankton harvest system, much higher attachment levels must be achieved in the ocean than what was done in this study. Bubble driven upwelling provides an alternative, but has several serious disadvantages.



# Table of contents

1 Introduction .....	1
1.1 Marine harvest at lower trophic levels .....	1
1.2 Calanus finmarchicus' potential as a commercial product.....	1
1.3 Copepod fishing: historically, today and in the future .....	2
1.4 Bubbleology .....	4
1.5 Use of bubbles and bubble plumes in water.....	7
1.6 Flotation .....	7
1.7 Upwelling.....	10
1.8 Aim of study.....	11
2 Materials and Methods .....	13
2.1 Experiment set-up .....	14
2.1.1 Big tank .....	14
2.1.2 Water circulation .....	15
2.1.3 Bubble generation .....	16
2.1.4 Air supply.....	18
2.1.5 Copepod insertion .....	18
2.1.6 Camera and lighting .....	19
2.1.7 Camera adjustment.....	20
2.2 Experiments.....	20
2.2.1 Pilot study.....	20
2.2.2 Attachment (big tank).....	21
2.2.3 Copepod-bubble interactions (small tank) .....	22
2.2.4 Stamina.....	23
2.2.5 Bubble driven upwelling .....	24
2.3 Data treatment .....	26
2.3.1 Image processing.....	26
2.3.2 Bubble size analysis .....	27
2.3.3 Computer software and Statistics.....	29

3 Results .....	30
3.1 Observations from pilot study .....	30
3.2 Attachment (big tank).....	31
3.3 copepod-bubble interactions (small tank) .....	35
3.4 Stamina.....	35
3.5 Bubble driven upwelling .....	38
4 Discussion .....	40
5 Conclusions .....	48
Acknowledgements .....	49
References .....	50
Appendices	
Appendix A. Attached bubble size in filtered and algae water .....	54
Appendix B. Gaussian distribution test.....	55
Appendix C. Copepod-bubble interactions .....	56
Appendix D. Repeated Stamina experiment .....	58

## ***1 Introduction***

### ***1.1 Marine harvest at lower trophic levels***

The human population of this world is growing rapidly and with this follows an increasing demand for natural resources. This applies to food more than anything. A growing demand of protein, in particular, has resulted in a novel interest in the lower trophic levels in the ocean. In the 1960's and early 70's a large scale krill fisheries in the Antarctic was started (Nicol & Endo 1999). Today this industry catches around 150-200.000 tonnes of krill every year, with a peak in 1982 of just over 500.000 tonnes, and it has been kept at this level for the last decades. The huge development that was anticipated when it first started has not yet happened and the harvest in the Antarctic is today limited by market demand rather than science based regulations ([www.ccamlr.org](http://www.ccamlr.org)). However, the krill fishery is being closely monitored by the Convention on the Conservation of the Antarctic Marine Living Resources (CCAMLR) who set precautionary catch limits each year (Nicol & Endo 1999). CCAMLR also monitors other aspects of the krill fisheries such as by-catch (Watters 1996). Hence the work of CCAMLR ensures that a future expansion of this industry will be done in a precautionary way.

### ***1.2 Calanus finmarchicus' potential as a commercial product***

Krill is not the only lower trophic level animal that has been considered for commercial harvest. *Calanus finmarchicus* is a copepod species found in great abundance along the north Norwegian coast and in the rest of the north Atlantic and Barents Sea (Tande 1991, Astthorsson & Gislason 2003). *C. finmarchicus* is one of the key species in these areas with a very large yearly production of biomass. However, only a small portion of the production, estimated to 10-20%, is utilised by higher trophic levels (Lalli & Parson 1997). The species overwinters in the deep waters of the open ocean as development stages CIV and CV but comes in to shallower areas in the spring to spawn (Tande 1982). The arrival of the copepods is closely related to the phytoplankton spring bloom (Astthorsson & Gislason 2003). The males are first to arrive around March while the females and copepodite stages CIV and CV are found in great numbers in May-June (Pasternak et al. 2001). At this time there are no longer any males to be found in the area. *C. finmarchicus* contains large amounts of lipids, mostly in form of wax esters (60-90 % of the total lipid content in CIV-V and females) and their fat content increases exponentially from developmental stage CI to CV (Kattner &

Krause 1987). Adult females often have a slightly lower lipid store than CV. The amount of omega-three polyunsaturated fatty acids (n-3 PUFA) is generally very high in *C. finmarchicus* as well in related species. Fraser et al. (1989) report measurements of 28 % n-3 PUFA (of total lipids) while even higher values are presented by others (Kattner & Krause 1987, Kattner et al. 1989). Because of the species low trophic position one can also expect much lower levels of organic pollutants and heavy metals than in e.g. cod liver or seal oil, which are used as food supplements by people especially during the dark months in the arctic. Hence, human health products is a potential market for this newly considered natural resource. The oil from *C. finmarchicus* has also been tested for use in salmon (*Salmo salar*) feed as an alternative to fish oil, with promising results. The salmon have no problems digesting the wax ester-rich oil and showed efficient deposition of n-3 PUFA in muscle and liver (Olsen et al. 2004). Not surprising, given that the majority of the marine food web, including planktivorous fish, rely on copepods as their food source. When processing the copepod raw material a protein and mineral-rich powder is also attained. This powder is marketed as a food ingredient, suitable for human as well as aquaculture use, and is reported to have a strong lobster-like flavour (www.calanus.no). The author can report that these copepods are quite tasty raw, straight from the ocean as well.

### ***1.3 Copepod fishing: historically, today and in the future***

Fishing for *C. finmarchicus* in Norway started in the 1950's in the fjords around Trondheim (Wiborg & Hansen 1974). At this time the copepods were caught from small boats using fine-meshed nets which were towed from the boat. Fishing took place in the evenings of May-June and the fishermen could catch a few hundred kilograms per night. The catch was frozen or preserved in other ways and sold as feed to experimental salmon farms in Sweden or for aquarium fish. In 1962 seven tonnes of copepods were caught. Later in the 60's trout farmers in Bergen started harvesting copepods for their fish, using stationary nets. The nets were anchored in fjords known to house large amount of copepods where the current was strong enough to bring the animals into the nets, but not tear the fragile nets apart. At the same time, 1967-68, the Norwegian Directorate of Fisheries did evaluations of new towable copepod trawls as well as mapping the distribution of calanoid copepods in the Bergen area. During their cruises they managed to catch up to 85 kg/hour or 7 kg/hour/m<sup>2</sup> when trawling off-shore (Wiborg & Bjørke 1969). In-shore the catches were generally much smaller, with occasional hauls of up to 40 kg/hour. During the following decade a more or less regular industry was



established with yearly catches of about 50 tonnes in the mid 1970's. After that, the copepod harvest business has been fairly inconspicuous. The fishing has continued at a low level of a few tonnes a year but without any technological developments.

In 2002, a new company called Calanus AS was established in Tromsø, Norway ([www.calanus.no](http://www.calanus.no)). Their objective was to restart and develop the copepod harvesting industry, including all steps of production from catch to processing and marketing. In cooperation with SINTEF and NTNU (Trondheim) and NCFS (Tromsø) new trawls have been developed and are now at a quality and efficiency sufficient for commercial use, at least to some extent. During this last season, 2008, catches of up to 8 tonnes per day were achieved, resulting in a total catch of 90 tonnes for the three weeks of the entire harvest period. Calanus AS is today the only business in Norway with a fishing permit for copepods. The permit is for research fishing and allows a catch of 1000 tonnes per year. The trawls so far have been intended for small and medium sized boats, up to 35 m. However, in order to reach the goal of full scale commercial harvest, fishing will have to be done with larger boats off-shore. One important aspect of this is the ability to freeze and store large amount of copepods on board the boat. If not frozen soon after harvest, the quality of the catch will deteriorate quickly (Wiborg & Hansen 1974). Moving the fishing area of copepods away from the shore is also desired from an ecological and resource management point of view. Firstly, people are afraid that copepod harvest in spawning areas of fish will result in food shortage for the fish larvae and fingerlings, since *C. finmarchicus* is a very important food source for higher trophic levels. Secondly, there is the problem of by-catch. When trawling in areas of fish spawning or larvae drift, one can expect that there will be a certain degree of by-catch of fish larvae and eggs.

All the harvest systems of today are based on filtration of water through very fine meshed nets, mostly of 0,5 mm mesh size. This is accompanied by several challenges in areas like hydrodynamics and material technology. Use of fine twines makes the equipment fragile and has to be reinforced with e.g. outer trawl nets of larger mesh size. The fine meshed materials also make an efficient water flow through the trawl harder to achieve. The net has a very low open mesh to trawl area ratio, a high solidity, compared to conventional trawls. At the time of the year most interesting for copepod harvest there is also large amounts of phytoplankton in the water. These will clog the net, thus reducing the water flow even more. A way to minimise the effect of algal clogging is to make the nets more elongated or even make a part of the net cylindrical before the tapering towards the back. Making the trawl cylindrical does

not only give a larger net area, as the elongated cone shaped ones, delaying the clogging effect. It also results in an oscillating motion of the trawl walls inhibiting phytoplankton attachment (Gjøsund 2006). Hydrodynamics of a fine meshed trawl like these are very different from conventional ones, and present even more challenges. The small dimensions of twines and mesh openings mean that we are operating at low Reynolds numbers, making the effect of viscous forces much more important (Mann & Lazier 2006). At such a small size scale the boundary layer around the twines have a significant effect on the water flow. This has an additive effect to the already low flow through the trawl because of its solidity.

As seen above there are a number of limitations to today's harvesting systems for zooplankton. Moving the harvest off-shore and to bigger boats will also mean larger expenses in e.g. fuel and man power, and thus greater need for cost efficiency. So, alternative approaches may be greatly needed in the future. Use of air bubbles may provide a solution. Bubbles are used for particle concentration in many different industries (1.5 Use of bubbles and bubble plumes in water). If this technique could be implemented on zooplankton in the ocean there would be a substantial increase in the efficiency of the harvest system. A towed bubble generation system can potentially lift a significant amount of the copepods up through the water column and concentrate them at the surface. A small trawl or surface skimmer can collect zooplankton at the surface from a water volume widely exceeding that of the trawl opening. In addition to its concentrating effect, the bubbles are hypothesised to reduce by-catch. Using right size bubbles may provide attachment and flotation to the target species more efficiently than other animals in the water, giving a cleaner catch. A problem in today's copepod fishing is by-catch of jellyfish, which with their digestive enzymes deteriorate the catch rapidly on board the boat. Large amounts of jellyfish also cause clogging of the nets while trawling, which results in great operational difficulties (Angell, pers. comm.<sup>1</sup>). Given their considerable differences in morphology from copepods there is great hope in excluding jellyfish from the catch with the help of bubbles.

### ***1.4 Bubbleology***

To fully understand and appreciate the concept of bubble flotation and a potential application on marine harvesting techniques one needs to be familiar with some of the basics in bubble science. In the literature there is a divergence in how to present bubble sizes, some use radius

---

<sup>1</sup>Personal communication: Snorre Angell, Calanus AS, NO-9272 Tromsø

while others insist on using diameter. This can be quite confusing, so I would like to point out that all bubble sizes in this study are given in radius. For bubbles that are not spherical their size is given as an equal spherical radius, see “Bubble size analysis” in materials and methods for further explanation. The definition of the term micro-bubbles also exhibits a lack of consistency among researchers, a nuisance that can create unnecessary agitation in discourses between fellow bubbleologists. When it is used in this document micro-bubble refers to bubbles with a maximum size of about 100  $\mu\text{m}$ .

Rise velocity of bubble varies mainly with size, shape, amount of surfactants (surface acting agents) and rise path (Bel Fdhila & Duineveld 1996, Ellingsen & Risso 2001, Patro et al. 2002, Tomiyama et al. 2002). In different water qualities the rise velocity varies greatly (Figure 1), especially in the size range of 500-2000  $\mu\text{m}$  (Patro et al. 2002). The velocity is greater in clean than dirty water (Maxworthy et al. 1996). A 700  $\mu\text{m}$  bubble typically rises at a speed of 35 cm/s in clean water while in dirty water this value can be as low as 10-15 cm/s (Figure 1). This is due to the formation of a surfactant cap on the aft side of the bubble (Patro et al. 2002). When this cap covers half of the surface area of a spherical bubble there is a sudden decline in the rise velocity (Bel Fdhila & Duineveld 1996).

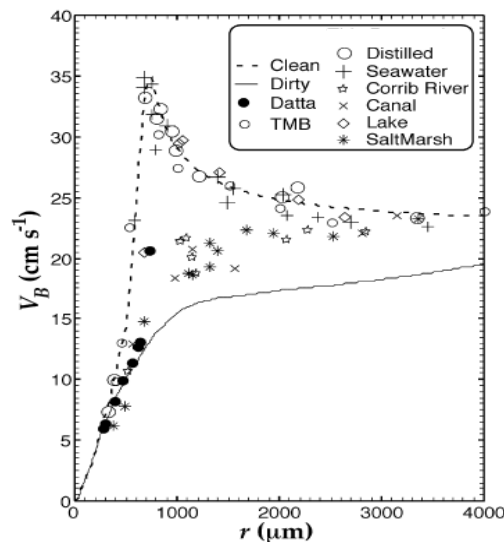


Figure 1. Rise velocity ( $V_B$ ) as a function of bubble radius ( $r$ ) for both modelled and measured data (Patro et al. 2002)

Small bubbles, i.e. micro-bubbles, have a shape very close to a sphere. However, as we move into larger size ranges they start showing tendencies of oscillation and taking more ellipsoid shapes. For bubbles of 1-2000  $\mu\text{m}$  their shape can be determined by the method of generation, e.g. different capillary tube diameters. This also affects their rise velocity. Wu & Gharib

(2002) report velocities of 10-20 cm/s for spheres and 25-38 cm/s for ellipsoids in clean water for the mentioned bubble sizes. These different shape bubbles also exhibit differences in rise path, zigzag for spheres and helix for ellipsoids, although one type can experience changes in stability and evolve into the other (Ellingsen & Risso 2001, de Vries et al. 2002).

As a bubble rises through the water it changes in size due to bubble-water gas exchange and changes in hydrostatic pressure. Even if the bubble is stationary it will change in size because of the osmotic transport of gas molecules through the bubble-water interface. Typically it shrinks as the gas moves out to the water, unless the water has a strong oversaturation of gas beforehand. This is the case in carbonated beverages where you instead have formation of bubbles. The gas exchange over the bubble surface decreases with the surfactant load of the water, due to the formation of organic skins. Rapid changes in bubble size can also be prevented by water pre-saturation of the air used to produce bubbles (Manley 1960). When a bubble rises through the water column it experiences a declining hydrostatic pressure. This causes the gas inside it to expand, making the bubble larger. The combined influence of decreasing hydrostatic pressure and bubble-water gas exchange has different effects on small and large bubbles. Because of the high surface-volume ratio, osmosis is dominating the size change in very small bubbles while it has a minute effect on larger ones. In practice, this means that when rising from great water depths tiny bubbles will diminish before they reach the surface. Larger bubbles will, on the contrary, grow in size as they rise (Figure 2).

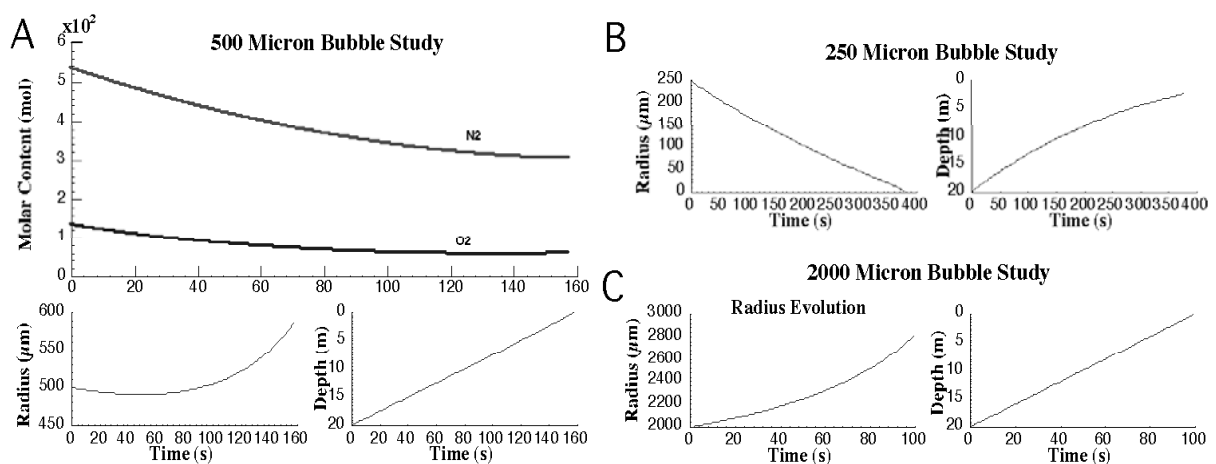


Figure 2. Size change of air bubbles rising through the water column. A 500  $\mu\text{m}$  bubble initially decreases in size due to outflow of air and then grows bigger from decreasing hydrostatic pressure (A). A 250  $\mu\text{m}$  bubble is more affected by the outflow of air and diminishes before reaching the surface (B). The larger 2 mm bubble continuously grows despite loss of mass,  $\sim 50\%$ , through osmosis (C). Figures are from model Ira Leifer for NRC project: “Harvesting zooplankton by bubble flotation”, described in Leifer et al. 2006).

### ***1.5 Use of bubbles and bubble plumes in water***

The use of air bubbles in water is in no way a new concept. There is a myriad of interesting applications available in different industries. Flotation uses small bubbles produced mainly with diffusers, porous materials or venture injectors, and electrolysis (Chen et al. 2002, Kawamura et al. 2004). It is used to remove particles during waste water treatment in sewage plants, mining and palm oil production as well as water recycling in land based aquaculture where it can also be used for aeration (Chen et al. 1992). As micro-bubbles rise up through the water hydrophobic particles like proteins or carbohydrates attach to them and are brought up to the surface where they are retained in the foam (Chen et al. 1992). The foam can then easily be removed with a skimmer.

The upwelling effect of bubble plumes is utilized in a diverse range of applications. Water treatment ponds and reservoirs can be de-stratified to facilitate desired bacterial activities or prevent deterioration of water quality due to anoxic conditions at the bottom and harmful algae blooms at the surface (Schladow 1993, Kim et al. 2006, Yum et al. 2008). Linear bubble plumes are used to prevent oil spills from spreading on the water surface in harbours as well as ice formation near hydraulic constructions and boats ([www.hydrotechnik-luebeck.de](http://www.hydrotechnik-luebeck.de)). A more detailed description of the mechanisms involved in these two different means of particles transport in water, flotation and upwelling, will be given below.

### ***1.6 Flotation***

The current study is mainly focused on flotation as a mean to bring copepods to the surface of the ocean. Calanoid copepods are slightly negatively buoyant. Flotation is achieved when bubbles are attached to the animals, thus giving them buoyancy. In addition to actually lifting the animals it is possible that attachment of bubbles inhibit their motility, reducing their avoidance efficiency. Interactions between bubbles and particles during the flotation process include three stages, collision, attachment and detachment. Hence, first the bubble and particle, in this case a copepod, must collide. The collision efficiency, or probability, is defined as ratio of real and ideal collision rate. It is mainly determined by the radius and velocity of the bubble and particle (Phan et al. 2003). Because the motion path of the particle and bubble have to intersect to result in a collision the bigger the radius the more likely the area to come in to contact. Also if there in no difference in velocity between the two they will never collide. As the particle approaches the bubble, or opposite, it will be affected by the

liquid flow around the bubble. The flow is asymmetric in front and behind of the bubble (Figure 3) with more compressed streamlines towards the front, a “bow wave”, and a turbulent wake behind (de Vries et al. 2002). This gives an outward flow at the bubbles equator which affects both the collision and attachment rates. Consequently, the area of potential collision is less than the entire frontal hemisphere of the bubble. This is referred to as the maximum collision angle. The motion of the particle will also as it approaches the bubble be affected by several other factors e.g. the particle mass influencing inertial and gravitational effects as well as their zeta-potential. The zeta-potential is a measurement of an objects surface electric charge and changes with  $Al^{3+}$ -ion concentration, pH and salinity of the water (Han et al. 2006, Myers et al. 1975). There is an increase in collision efficiency when the zeta-potential of particle and bubble are of opposite charge.

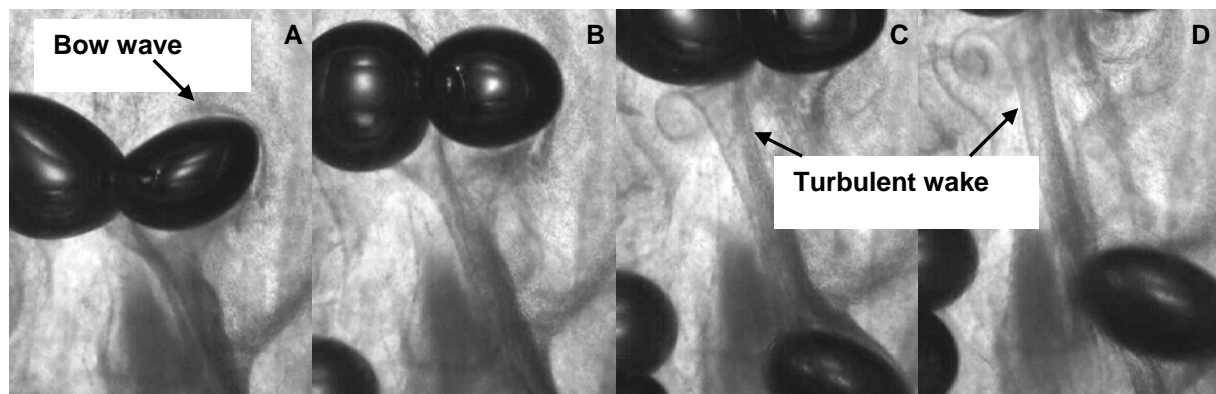


Figure 3. Liquid flows around rising bubbles showing formation of a bow wave in front of the bubble (A) and the turbulent wake behind it creating vortices (C, D). Algae, *Skeletomena costatum*, were used as flow tracers. Time between each image is 7 ms.

The second step towards successful flotation is attachment. As the particle approaches the bubble, the particle deforms the bubble and slides along the surface until it reaches the maximum collision angle. The duration of this is referred to as the contact time. The attachment mechanism can be described in three steps which together make up the attachment time (Nguyen et al. 1997):

- Thinning of liquid film to critical thickness
- Rupture of liquid film and formation of three phase contact
- Expansion of the three phase contact to form a stable aggregate

For the attachment to be successful the attachment time, also called incubation time, must be shorter than the contact time (Phan et al. 2003, Sven-Nilsson 1934).

The third factor that affects the outcome of the flotation process is detachment. Of course the lowest possible detachment rate is desired. The main adhesive forces preventing the three-phase contact area to diminish are:

- Capillary forces
- Hydrostatic pressure force on the area enclosed by the three-phase contact
- Buoyancy of the particle volume immersed in the liquid phase

The most important forces working for detachment are the particle weight and the turbulent inertial forces (Phan et al. 2003).

An additional factor likely to affect the overall attachment rate is the presence of surfactants in the water (Malysa et al. 2005). One potential group of such surfactants is algal exudates. High levels of dissolved and particulate organic carbon (DOC, POC) are known to increase the “stickiness” of the water (Mopper et al. 1995, Zhou et al. 1998). A range of marine organisms exude polysaccharides, among these are phytoplankton, especially diatoms and the haptophycean *Phaeocystis* spp, as well as bacteria, ascidians and bivalves (Alldredge et al. 1993, Heinonen et al. 2007). Eventually, these polysaccharides, along with other organic carbon compounds in the water form transparent exopolymer particles (TEP) which are found in high abundance and are important for particle aggregation in the ocean, e.g. formation of marine snow (Alldredge et al. 1993, Passow et al. 1994, Passow and Alldredge 1995). TEP is found in high concentrations during diatom blooms and are largely responsible for the flocculation of these algae, causing them to sink out of the euphotic zone. They are hence often responsible for termination of phytoplankton blooms. TEP is also efficiently produced by bubbling of the water column (Kepkay & Johnson 1989, Zhou et al. 1998). Described in a simple manner the bubbles pick up small organic compounds which are then brought up to the surface and remain fixed together as TEP after the bubble is gone. The idea for the current study is that sticky surfactants that evidently help aggregate and float smaller particles may also facilitate the flotation of larger particles such as copepods. In a study by Malysa et al. (2005) on bubble attachment to larger hydrophobic objects, Teflon plates, the attachment rate was proven to increase with the addition of sticky surfactants. They also reported that the roughness of the surface and presence of micro-bubbles influenced the attachment rate. Parts of the flotation experiments in this study are therefore done with the addition of algae, *Skeletonema costatum*, in the test tank. *S. costatum* is a phytoplankton species of the group diatoms which is known to contain many polysaccharide exuding species (Alldredge et al..

1993). At the time of the year when harvest of *C. finmarchicus* is at its peak there are often large amounts of phytoplankton in the water. If it is shown that the presence of certain species of micro algae enhance the flotation process, a planning of the harvest to certain areas and time periods may give more efficient collection with the new bubble based harvest system.

### **1.7 Upwelling**

When bubbles move together in a plume they behave differently than on their own. As shown in the previous chapter, single bubbles create turbulence as they rise through the water (de Vries et al. 2002). A bubble moving in the same mass of water as other bubbles will be affected by the wake of these. As a result bubbles in a plume will generally exhibit greater rise velocities than single ones. When a stream of bubbles is released into the water column it will drag the water with it vertically, creating an upwelling flow (Figure 4). If this happens in a homogenous water column, water from the surrounding area will be sucked into the plume, entrained, and brought up to the surface (Asaeda & Imberger 1993). As it reaches the surface it changes direction and moves horizontally away from the plume core, so called outwelling.

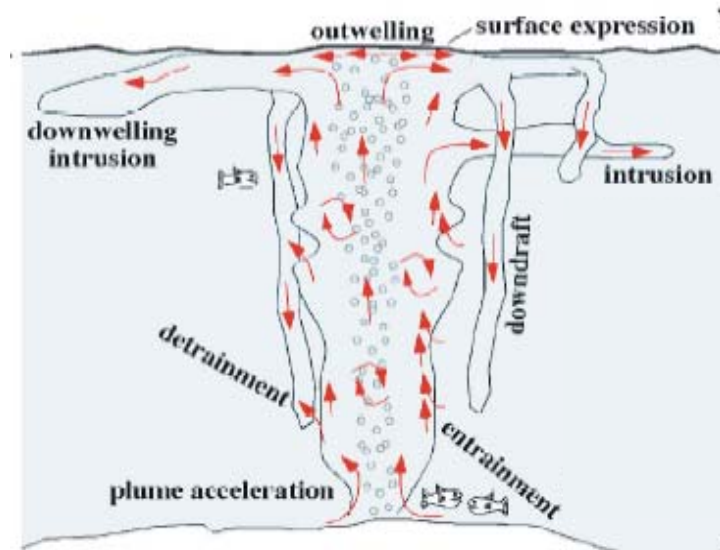


Figure 4. The major flow patterns involved in bubble driven upwelling (Leifer et al. submitted 2008, modified by author)

In a stratified environment the flow patterns become more complex (Figure 4). Still there is entrainment of water, but as the heavier water is lifted it reaches a point where its negative buoyancy becomes too great, resulting in detrainment and intrusion (Asaeda & Imberger



1993). Detrainment will have a significant effect on the overall upwelling, as upwelling water and contained particles will be lost through intrusion on the way up (Schladow 1992, Leifer et al. submitted 2008). The depth at which intrusion occurs depends on the strength of the stratification, and also the bubble size in the plume according to Sato & Sato (2001). Bubble driven upwelling will definitely have an effect on the flotation process of zooplankton. As water is lifted vertically by the bubble plume organisms in the water will also be lifted. However, these aspects will be discussed more in the designated chapter.

### ***1.8 Aim of study***

This study is part of the NRC (Norwegian Research Council) funded project “Harvesting zooplankton by bubble flotation” (project number 178421/S40). The project is lead by SINTEF Fishery and Aquaculture and aims to find a novel environment friendly method of harvesting copepods in the ocean. The idea is to, with the help of air bubbles, bring the target species up to the ocean surface, hence minimising the by-catch of other marine organisms. Concentrating the copepods at the surface should also enable a more energy efficient method of collection.

The primary focus of the current study is to make an initial evaluation of the potential for bubble flotation to improve the efficiency in a copepod fishery. It is achieved by experimental investigation of the most crucial factors influencing a flotation process. The results are also intended to provide a basis for development of large scale field trials within the research project. Initial focus of the study is presented in points 1-3 below. After preliminary analysis of the acquired data the decision was made to expand the study to also cover the issues in points 4 and 5. The study has the following objectives:

- 1) Find the optimal bubble size for maximum bubble-*C. finmarchicus* attachment efficiency and determine the attachment rate
- 2) Measure the flotation effect on *C. finmarchicus* from attached bubbles
- 3) Determine whether addition of algal exudates affects attachment
- 4) Study the behavioural and physical interactions of *C. finmarchicus* and bubbles
  - a. Visualisation with close-up, high-speed imaging
  - b. Stamina measurements on escape jumping
- 5) Quantify vertical water transport (upwelling) induced by bubble plumes of different air flow and bubble size.

Finding the optimal bubble size for attachment to *C. finmarchicus* will give the answer to what bubble producer to consider for the bubble harvest system. Different bubblers give different bubble size distribution (2.1.3 bubble generation). Using a narrow range of bubble sizes may decrease the amount of by-catch. The theory is that organisms of other shape and size will have an optimal bubble size range for attachment differing from that of the target species. Hence the unwanted organisms will not be affected by the flotation process to the same extent. The flotation effect of attached bubbles on the copepods will be measured through their rise velocity. The hypothesis is that the rise velocity of the animals will increase with their attached bubble volume. This is tested with regression analysis.

Literature on the surface chemistry of bubbles, see “flotation” below, indicate that it should be possible to increase the attachment efficiency with algal exudates. To test this, attachment experiments are done in both filtered seawater and with the addition of the diatom *Skeletonema costatum*. Comparisons are made on attachment rates as well as size distribution of attached bubbles.

Knowing how the copepods react to the presence of bubbles is important in order to understand the mechanisms involved in the flotation of live animals. Do they try to avoid the bubbles or are they passive? These issues are likely to affect the attachment rate and thus the efficiency of the flotation process. For this purpose a small scale attachment experiment was set up in a 30-litre aquarium, enabling high-quality close-up visualisation of bubble-copepod interactions. *C. finmarchicus* along with other related species are known to possess the ability of performing fast and lengthy escape jumps. *Acartia tonsa* reacts to both hydrodynamic and light stimuli by escape jumps at a velocity of up to 80 cm/s (Buskey & Hartline 2003). *C. finmarchicus*' jumping behaviour may potentially have a significant negative effect on the attachment efficiency as well as the detachment rate. However, a small animal like this must have limitations in stamina, i.e. for how long a period they can keep jumping before they become passive. For what reason do they eventually stop, loss of stimulus sensitivity or energy depletion? A stamina experiment was designed to test this, here the copepods were stimulated to jump and the activity time was measured.

In addition to flotation the copepods can potentially be brought to the surface by a separate mechanism: upwelling. Although this study is focused on the flotation mechanism it also includes a quantification of bubble driven upwelling flow. Upwelling velocity of the vertically

transported water mass is measured in a tank, using fluorescent dye as a tracer. Different bubble sizes are tested and compared as well as the relationship between air use and attained upwelling velocity.

## ***2 Materials and Methods***

The current study presents a novel approach to zooplankton harvest in the ocean. Very little previous published work is therefore to be found on the subject. Consequently, the approach has been to merge several traditionally separated science disciplines, and a lot of effort has been put into learning new fields of science as well as designing equipment and developing adequate methodology. Eventually the trial and error approach resulted in several functional methods for investigating the potential of a copepod harvest system based on bubble flotation. The outline of the practical effort in this study is presented in Table 1. The majority of the experiments were carried out at SINTEF Sealab (Trondheim). In addition, eight weeks from mid April and onward were spent at the University of California, Santa Barbara (UCSB) learning the basics of bubble science and digital image analysis under supervision of Dr. Ira Leifer.

Table 1. The practical work in the study was carried out during five time experiment periods from May 2007 to August 2008. The experiment periods are referred to in the text as Exp I-V for reader guidance.

Experiment period (Exp)	Time period	Location	Activity
I	22 May – 6 June 2007	SINTEF Sealab, Trondheim	- Equipment fabrication and assembly of big tank - Pilot study
II	20 - 31 August 2007	SINTEF Sealab, Trondheim	- Improvements on big tank set-up - Copepod-bubble attachment (big tank) - Copepod stamina
III	25 January – 22 February 2008	SINTEF Sealab, Trondheim	- Development of small tank set-up - Copepod bubble interactions (small tank) - Copepod-bubble attachment (big tank) - Upwelling (big tank)
IV	7 - 11 April 2008	SINTEF Sealab, Trondheim	- Upwelling (big tank)
V	14 – 15 August 2008	NCFS, Tromsø	- Copepod stamina

## 2.1 Experiment set-up

### 2.1.1 Big tank

The large experiment tank is referred to in this study as the “big tank”. It consists of four vertically stacked sections (Figure 5). The base section is a 30x30x30cm cube made with stainless steel plates that are welded together. The top side is fully open (30x30cm) to the adjoining sections. In the floor of the base section there is a 4cm circular opening that works as an in/outlet for water. On the outside this has a T-connection where one opening is fitted with a ball valve and a 1 inch hose leading to the drain. The other opening can be connected to a peristaltic pump (2.1.2 Water circulation) to create circulation in the tank. The bottom section is also equipped with a horizontal semi-extractable pipe, 125mm in diameter, working as a sluice (Figure 5 & 7). This sluice enables access to the bubble generator (2.1.3 Bubble generation) without emptying the tank of water and disassembling it. The sluice pipe is made of aluminium and coated with a layer of black paint protecting it from corrosion. The centre part of the pipe is modified into a platform with threaded holes for fixing bubble generators or other equipment inside the tank. The front end of the sluice pipe is sealed off with a circular, 5 mm thick stainless steel plate bolted to its flange. This plate has several built-in entry points for air, water, electrical cables or whatever needs to be connected to devices inside the tank. The bottom section is equipped with feet bolted to the floor, raising it 10 cm off the ground by.

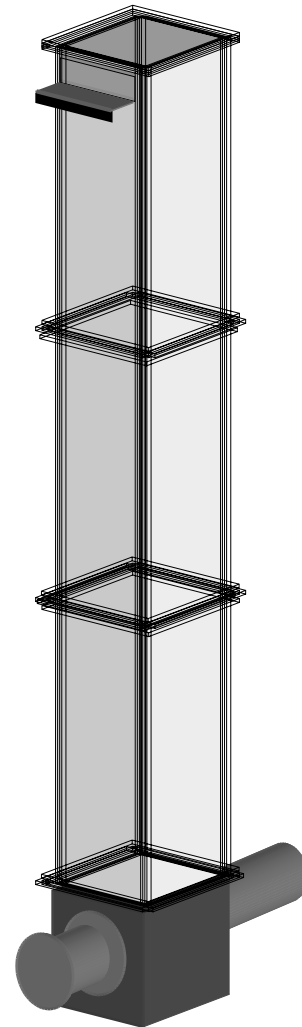


Figure 5. Schematic drawing of the large experiment tank (big tank), complete with all four sections.

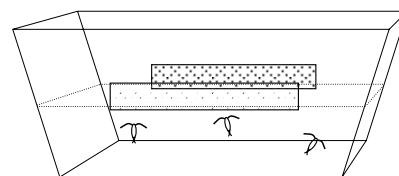


Figure 6. Schematic drawing of the filter unit for overflowing water in the big tank.

On top of the base section, the tank can be built by mounting one, two or three equally tall, see-through sections, approximately 1m each in height, giving the tower a maximal total height of 3,5 m. Two of these three sections are identical. They are made up of a welded aluminium frame holding triple paned hardened glass windows on all four vertical sides. The use of triple paned glass eliminates condensation when doing experiments with cold water in the tank, a necessity for good image quality. The glass is fitted to the frame from the inside with semi-hard rubber seal and silicone in between. Using a too soft seal between the window and the frame will give the glass room to move due to hydrostatic pressure once the tank is filled with water. This can lead to cracks in the sealant as the glass panes separate from each other in the corners of the tank, resulting in massive leakage.

One of the see-through sections is slightly different than the other two. On one side the glass ends approximately 10cm from the top leaving an open gap, which is fitted with a ledge. Underneath the ledge there is a sink containing a filtering unit. The filtering unit consists of a plastic tub which has two openings covered by 200 µm netting (Figure 6). Its purpose is to retain floated particles during water circulation.

The four sections are stacked on top of each other with hard rubber seals between the flanges of each joint, and bolted together with 16 bolts. Interior of the flanges are also softer weather strips to fill the gap that would otherwise form between the glass panes of two sections. This minimises the areas for the test animals to hide or get trapped (Figure 6). The top of the tank is fitted with a removable lid to prevent contamination of the inside if the tank.

### ***2.1.2 Water circulation***

The tank was filled with water from the top with a hose and emptied through the in/outlet in the floor of the bottom section. Water was taken in from the Trondheim fjord and filtered (sand filter). If desired, it was possible to re-circulate the water in the tank at a variable speed. The water was then pumped into the tank through the inlet in the bottom section by a peristaltic pump, a Grundfos DME 375 with flow capacity of 0,47-375l/h. When the water reached the top of the tank it overflowed into a sink and ran through a hose to a reservoir, made from a 25 litre polyethylene canister. From the reservoir the water went back into the pump. The type of hose used for the circulation system was chosen because it should not desorb any toxins or surfactants.

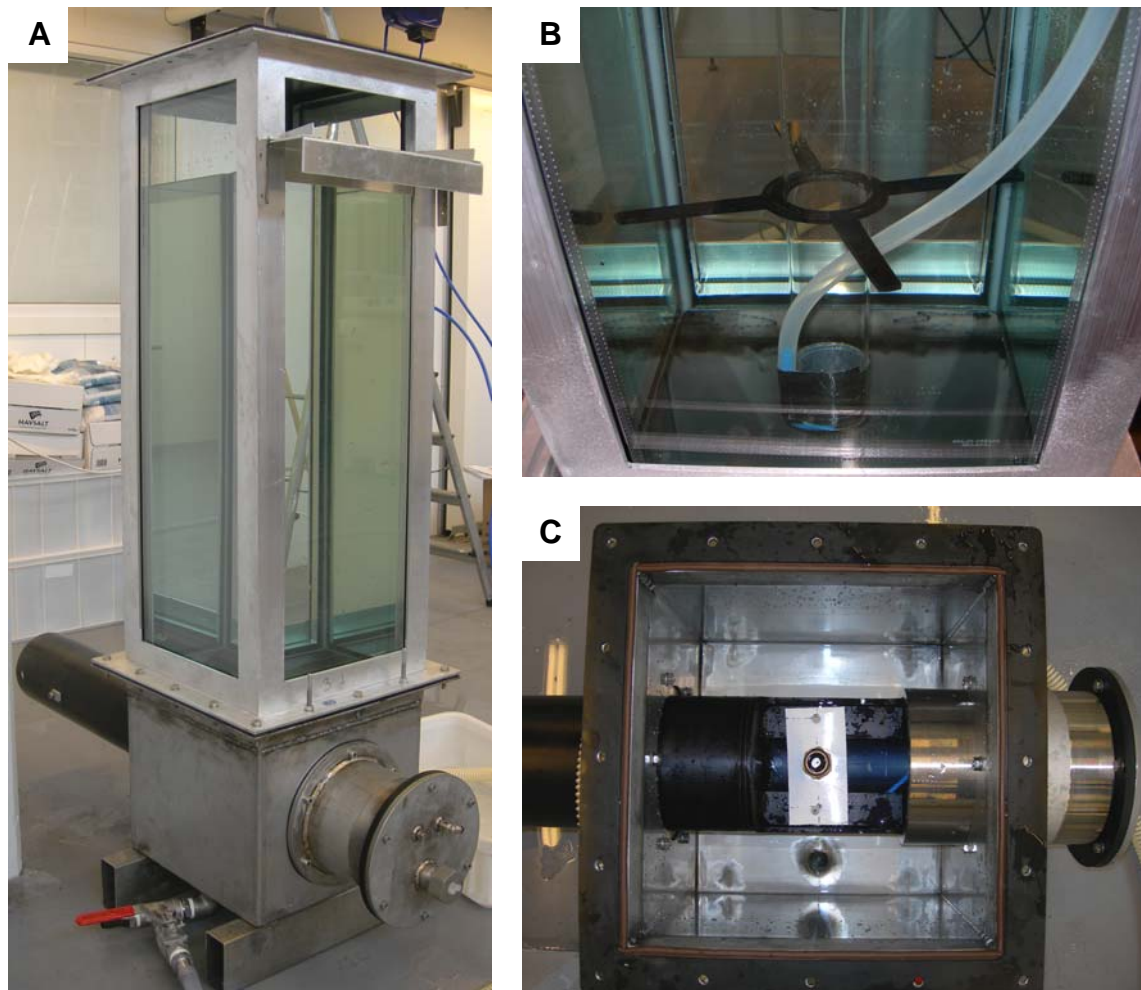


Figure 7. Features on the big tank: top and bottom sections mounted together (A), copepod insertion system with silicone tube leading the animals into the glass tube where they are forced to interact with the bubbles (B), and internal view from above, of bottom section, note porous plate bubbler fitted in sluice pipe (C).

### **2.1.3 Bubble generation**

Two different systems were used for generating bubbles, glass capillary tubes and porous metal plates. The capillary tubes were made by heating Pasteur pipettes over a Bunsen burner. The pipette was heated at the thinning part. As the glass softened it could be elongated, which narrowed the inner diameter. It was then cut at the narrowest point, by filing a small cut with very fine glass cutter and then breaking it. Capillary tubes are very well suited for producing uniformly sized bubbles, but getting a clean straight cut is crucial for a good bubble formation. (Palanchon et al 2003). With some patience tubes can be made narrow enough to generate very small bubbles, less than 50  $\mu\text{m}$  in radius. But they are very fragile and the thinner the point is, producing smaller bubbles, the more fragile they become. Also, a single tube can only produce bubbles at rather low densities. Capillary tubes were used in all the small tank experiments, producing bubbles in the size range of approximately 50-1000  $\mu\text{m}$ . They were

also used in the big tank to make larger bubbles, mainly 50-700  $\mu\text{m}$ . Here three capillary tubes were used together to produce more bubbles.

The porous plates used to generate bubbles in this study are commercially available in a wide range of metals and alloys. They are industrially produced by sintering metal granules. The ones used in the current study were stainless steel, media grades 0,2; 0,5; 2; 20 and 100. They are referred to as P0,2-100 bubblers in the text. The media grade is an indication of the pore size, derived from its particle removal efficiency when used for filtration. The pore size also affects the bubble size distribution when used for sparging. Porous metal plates can be used to produce a wide range of bubble sizes. However, compared to capillary tubes a porous plate of a given media grade produces a wider spectrum of bubble sizes. The size distribution can be controlled to a certain degree, by applying a water flow across surface where the bubbles are formed. The flowing water helps to decrease the size by cutting off the bubbles from the surface before they have time to build up. Porous plates were the preferred means of bubble generation for the big tank experiments as they could easily produce bubbles at high densities. The actual bubbler was made in two different versions. In the first version the porous plate was placed in the 1 inch end of a 1 to  $\frac{1}{2}$  inch brass reducing coupling and held in place with a 1 inch double male pipe thread fitting. Rubber seals were placed on both sides of the plate to prevent leakage (Figure 7). This version was fitted with a flushing system to enable control of bubble size. The second version was made by fixing the porous plate, using epoxy, on top of a cap meant for 1 inch brass plumbing pipes. A hole, slightly smaller than the plate diameter had been drilled in the cap before hand to let the air through. The cap with the porous plate could then be threaded onto a male brass coupling held by a plastic plate which in turn was mounted in the designated area in the tank. The other end of the coupling was converted to the smaller dimension of the air supply system.

For very small bubbles, plumes of purely  $<50 \mu\text{m}$  bubbles, electrolysis was considered and tried in small scale tests. However it was not found suitable for use in seawater. The main issue was formation of insoluble salts, reducing water clarity and hence image quality. In fact, electrolysis is used as a purification method during brine based salt (NaCl) production, where mainly magnesium and calcium are removed by precipitation (electrochem.cwru.edu).

### 2.1.4 Air supply

Air for bubble generation was supplied from an in-house compressor commonly used for high pressure air tools etc. The compressor delivered air at a pressure of 6 bars. This was more than what was needed, or could be used safely for that matter, for any of the experiments. The pressure had to be reduced and accurately controlled. For this purpose a flow control system was constructed and connected to the air supply line (Figure 8). The system was mounted on the side of the big tank and connected to the bubble generator with a short length of pressure resistant air tubing, 6 mm inner diameter. In order to accurately control the size and number of bubbles emitted, it is crucial to minimize the volume of air and the length of tubing between flow controller and bubbler. The more air between them the slower the response from the bubble generator. As the air entered the flow control system the starting pressure of 6 bar was reduced with a regulator to a more manageable and instrument safe 2,5 bar. The air flow was then controlled with three parallel-connected rotameters (Krohne DK800) of different scale range (8, 40 and 250 l/h). The outgoing pressure was monitored with a pressure gauge placed after the rotameters. Before entering the tank the air passed through a check valve preventing back-flow of water into the control system. Each end of the system was also fitted with a ball valve.

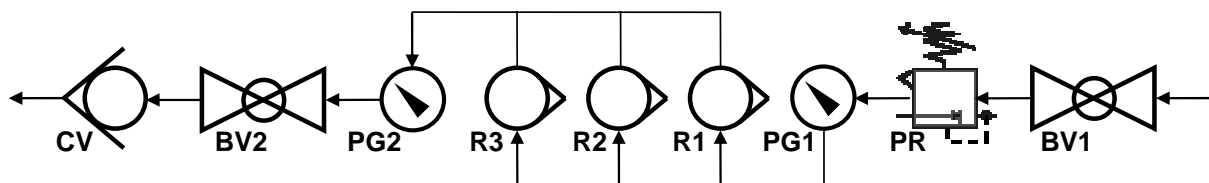


Figure 8. Schematic drawing of the air flow control system: Air coming from the compressor enters from the right and then leaves the system on the left, where it goes to the bubbler inside the test tank. BV: ball valve, PR: pressure regulator, PG: pressure gauge, R: rotameter, CV: check valve. Rotameters 1-3 with different scale range 8, 40 and 250l/h respectively.

### 2.1.5 Copepod insertion

During the experiments it was necessary to force the animals into contact with bubbles. If the copepods had the opportunity to escape the bubble plume they did. In the big tank this was done by confining the animals to the space inside a glass pipe in the centre of the tank (Figure 7). The pipe was 75 cm long with a diameter of 5 cm and was suspended by strings from the top of the tank. The lower opening was placed approximately 20 cm above the bubble generator making it possible to enclose the entire bubble plume at low to moderate air flows. The animals were inserted via a funnel at the top of the tank and brought down to the lower opening of the glass pipe through a 10 mm silicone hose (Figure 7 & 10). The silicone hose



ended in a bend around the edge of the glass tube injecting the copepods at an upward angle straight into the centre of the bubble plume. They then travelled upwards along the length of the tube getting hit by and hopefully attached to the bubbles. Eventually they reached the upper opening of the tube where they passed through the field of view of the camera enabling us to take pictures.

#### ***2.1.6 Camera and lighting***

The camera used in the study was a Basler A602f (Figure 9), with a 1/2 inch monochrome 656 x 481 pixel CMOS sensor (complementary metal oxide semiconductor). It has a guaranteed speed of 100 fps (frames per second), higher if not the entire field of view is recorded, using so called partial scanning. The camera was connected via FireWire 400 (IEEE 1394 interface) to a PC where it was controlled through the computer program LabView. The program enables control of shutter speed, gain and area of interest (partial scanning). The frame rate was controlled with an external trigger in form of an oscilloscope. The images were stored as 8-bit bitmap files directly onto the hard drive of the computer. The storing process was on- and offset by remote control. This enabled the experimenter to control the camera while keeping a close eye on the proceedings in the tank. With a frame rate of 2-300 fps it was important to limit the length of image sequences stored to that of actual interest. Therefore when taking images of copepods the camera was started when there was an animal moving into the field of view and stopped when it had left. Otherwise the amount of useless data would have built up rapidly.

Two different lenses were used. One was a Techspec silver series 0.16X telecentric measuring lens with fixed focus, product no. NT56-675 (Figure 9). The other one was a 55 mm FL partially-telecentric video lens with manual focus, product no. NT52-271, both from Edmund optics. With the telecentric lens the camera had a field of view of 40x29 mm. With the 55 mm lens and a zoom-extender it was possible to narrow it down to 7,4 x 5,6 mm for the full field of view. When used for the big tank the camera was mounted on an external aluminium frame, allowing it to be fixed at any desired position along the height and width of the tank. For the small tank experiments the camera was placed on a tripod.

All imaging was made with backlighting. The lighting consisted of four diode arrays fixed on a computer fan for cooling (Figure 9). In front of the arrays was a two step diffuser. First the

light was scattered by prisms and then mellowed by a sandblasted sheet of acrylic. The lights and fan were powered by a DC-power source with variable current and voltage, enabling control of light intensity.



Figure 9. Camera with telecentric lens (A) and LED-array used for backlighting (B), mounted on a computer fan for cooling.

### ***2.1.7 Camera adjustment***

When setting up the camera before each experiment a certain process was followed to optimize image quality. Firstly, the area of the tank window in front of the camera was cleaned. On the outside the glass was washed with window soap and wiper. Bubbles stuck to the inside of the glass were removed with a telescopic window wiper from the top of the tank. Then the camera was focused to the correct point inside the tank, in the middle of the bubble stream. This was done by turning the lights down low and opening the aperture of the lens as much as possible. This narrowed the depth of field. A calibration ruler for microscopes was suspended from the top of the tank to the desired point of focus. With the ruler in focus in the field of view the camera was fixed in the correct position, or for the model where it was possible the focus was set on the lens. With the camera set to the correct focal length the lights were increased to their maximum and the aperture closed down to give the images a balanced brightness and a wider depth of field. A few images of the ruler were then recorded and later used for calibration during the analysis of bubble size distribution.

## ***2.2 Experiments***

### ***2.2.1 Pilot study***

When most of the elementary fabrication and construction of the equipment was finished in the beginning of June 2007 a small scale pilot study was carried out (Table 1: Exp I). Only the two bottom sections of the big tank were used with a porous plate bubbler installed. Copepods

were injected into the bubble plume with a pipette and notes were taken on their behaviour in the presence of bubbles. Notes were also taken on the copepod-bubble attachments that were observed. These preliminary tests were done both with filtered sea water and with added algae. The results from the pilot study are of a purely qualitative level and were used as a basis for the outline of the main experiments (Table 1).

### **2.2.2 Attachment (big tank)**

The big tank was primarily used to determine the optimal bubble size for attachment to *Calanus finmarchicus*. Experiments were performed both in August 2007 and February 2008 (Table 1: Exp II-III). The initial idea was to force copepods and bubbles into physical contact for a period of time and then measure the size of the bubbles that were attached to the animals (see 2.1.5 Copepod insertion). The experiment was done using four different bubblers to acquire data from a wider range of bubble sizes. The porous plate bubbler was used with media grade 0,2; 0,5 and 2 plates and the capillary tube bubbler with one set of three glass tubes. Together the four bubblers covered a size range from close to zero to about 700  $\mu\text{m}$  radius, with occasional larger bubbles. All four bubble size cases were tested in filtered seawater as well as with added algae. The algae, *Skeletonema costatum*, were added, at a concentration of ca. 1000 cells/ml, to increase stickiness of the water and hence increase the copepod bubble attachment efficiency. The experiments were also run with lower levels of algae, ca. 300 cells/ml, using only the P0,2 bubbler. The bubbler was situated 20 cm above the floor of the tank, the glass tube at 40-115 cm, camera at 120 cm and water surface at 240 cm (Figure 10). The water temperature was kept between 12 and 14 °C, i.e. it had a temperature of 12 when it entered the tank and replaced before rising past 14 °C. The air temperature in the laboratory was ca. 17 °C.

The animals were forced into contact with bubbles for the duration of their journey through the 75 cm glass tube. When they exited through the top of the tube they were caught on camera. The image series were analysed for size of attached bubbles, size distribution of bubbles in plume and rise velocity of copepods (2.3.2 Bubble size analysis). In order to investigate the lifting effect of attached bubbles, the rise velocity of the copepods was plotted against their level of bubble attachment to see if there was any correlation. The attachment per copepod is presented as the spherical diameter equalling the combined air volume of all bubbles attached to that copepod.

### 2.2.3 Copepod-bubble interactions (small tank)

The small tank experiments (Table 1: Exp III) were done in a 30-litre aquarium. This aquarium is generally referred to in the text as the “small tank”. Inside the tank two different set-ups were organised for close-up studies of copepod-bubble interactions (Figure 10). For extreme close up imaging a 10 x 10 x 50 mm enclosure was made with three pieces of acrylic. The pieces were fixed together at a 90 degree angle and attached to the inside of the glass of the tank. The middle piece was put in slightly elevated from the others leaving a gap between it and the floor. The purpose of this gap was to get a capillary bubbler into the enclosure. The copepods were then inserted from above with a pipette. This set up was mainly used to get good quality extreme close up imaging of copepods with attached bubbles.

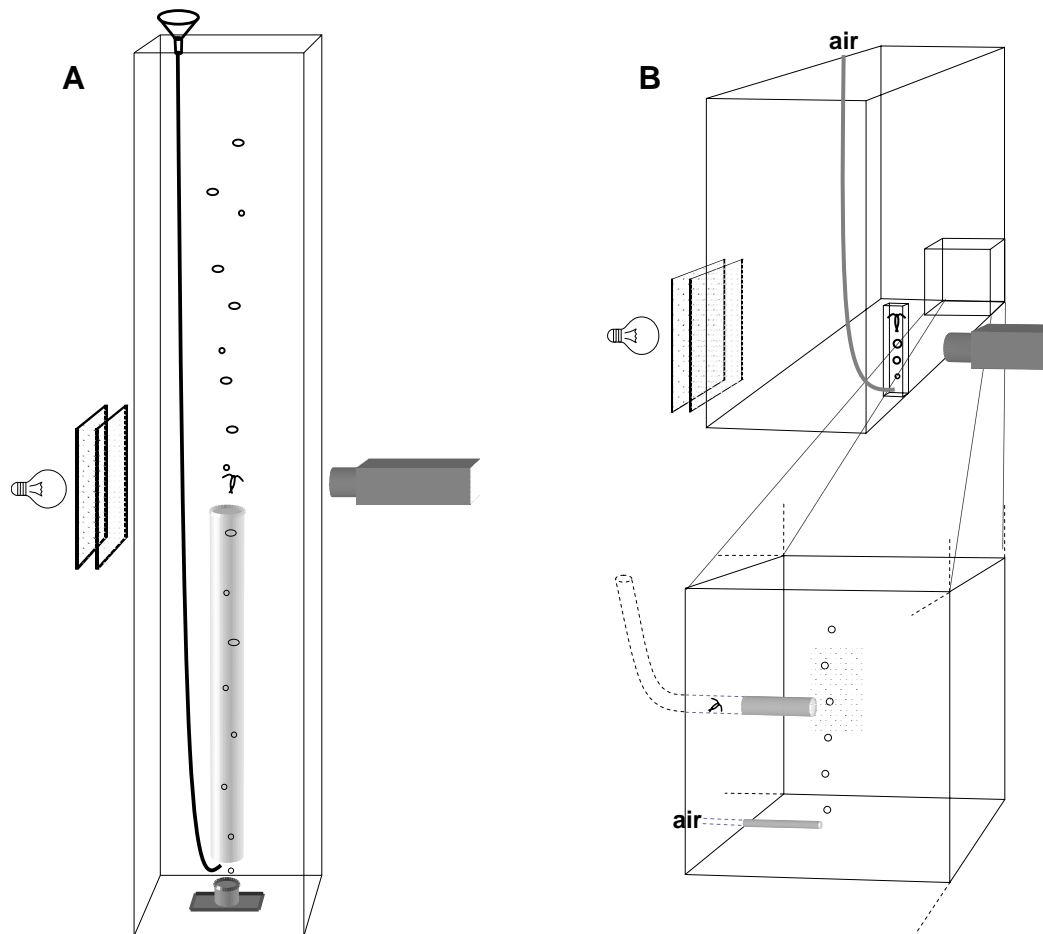


Figure 10. Schematic drawing of the imaging set-up for attachment experiments in large (A) and small (B) tank. The copepods were inserted in a funnel at the top of the tank and sent, together with the bubbles into a vertical glass tube. Bubbles became attached to the animals as they travel up the tube and were caught on camera as they exit the tube (A). The entire small tank with camera and lights set up for extreme close up imaging in 10 x 10 x 50 mm enclosure (B upper panel). Detail drawing of set up for close up studies of copepod-bubble interactions, shadowed area indicating field of view of the camera (B lower panel).

The second set-up in the small tank was used to study copepod behaviour when coming into contact with bubbles as well as the attachment rate and mechanism (Figure 10). Here a 100 x 100 x 100 mm enclosure was made by putting up two pieces of acrylic at a 90 degree angle in the corner of the tank. A hole was drilled in the middle of one piece in order to fit a flexible silicone tube through it. The tube had one opening in the centre of the enclosure and the other just above the water surface outside the enclosure. A second opening was made in the same piece of acrylic at the bottom straight down from the first hole. This opening was meant for the capillary bubbler. With the bubbler on and placed in the correct position a stream of bubbles was created just in front of the opening of the silicone tube. The copepods were inserted with a pipette into the tube and pushed slowly towards the opening and the bubbles by injecting additional water into the tube. As an animal entered the bubble stream the camera was triggered by remote control and an image sequence was recorded at 200 fps until the copepod left the field of view. Later, the images showing copepod-bubble interactions were analysed for bubble size, anatomic location of contact, behavioural and physical response and whether or not there was attachment.

#### ***2.2.4 Stamina***

Apart from the small tank experiments a separate behaviour study was done with the copepods (Table 1: Exp II, V). From observations during earlier experiments it seemed the most common cause for attached bubbles to detach was the animals' escape jump. In addition the copepods showed tendencies to make such jumps in response to larger bubbles. In order to find out if their jump behaviour might affect the bubble attachment efficiency a stamina experiment was developed. The idea was to test how many jumps the copepods could perform before they were exhausted. Because of the restricted mobility of a bubble generator a 10 cm glass rod (4mm in diameter) was chosen as the stimulus.

Prior to the experiment the copepods were kept in a 100 litre aquarium at a water temperature of 16°C. Unfiltered sea water was used in the tanks, providing the animals with a natural supply of food particles. In preparation of each experiment run copepods were taken from the tank and put individually in three one litre glass beakers filled with freshly tapped seawater. The beakers were placed in a row in a white polystyrene box, covered with black plastic and left to acclimatise for 20 minutes. The polystyrene box was chosen because it would help to keep the temperature at an even 11°C and provided a white background making it easier to

follow the animal visually. The whole polystyrene box was covered with black plastic to minimise any jump inducing stimuli during the acclimatisation period. The experiment was started by removing the plastic from the first beaker, keeping the other two covered from any external disturbance. Using the glass rod, the copepod was stimulated to make escape jumps. Often, the animals jumped away already as the stick was closing in on them. But sometimes the stick had to come into physical contact to result in an avoidance response. The copepods were chased and poked repeatedly until no reaction was obtained. No reaction was defined as three successive stimulations not resulting in escape jumps. The number of jumps was counted and the time from first to last jump was recorded. The experiment was repeated three times with the first five individuals with a resting time of approximately 20 minutes between repetitions. Then the entire experiment was repeated with fresh copepods. The reason for repeating the experiment several times using the same copepods was to find out if differences in stamina were individual or just random, i.e. if each individual responded at a similar level in all repetitions. Also, this data could be used to see if there was a change in response from one run to the next, e.g. declining number of jumps due to energy depletion or loss of sensitive to the stimulus. Sex and developmental stage were noted for all animals.

### ***2.2.5 Bubble driven upwelling***

In order to study and quantify the bubble driven upwelling a separate experiment was set up for the big tank (Table 1: Exp III-IV). The idea was to create an upward flow of water along the centre of the tank by running the bubbler continuously. The bubbler was run at a certain air flow and pressure for about five minutes to get a steady state circulation in the tank. The experiments were performed with a fixed volume of water not reaching the top of the tank and the overflow. This way, a circulation pattern was formed with an upward flow of water along the central vertical axis of the tank and an equal downward flow in the peripheral parts. A plastic tube was inserted vertically along one of the corners inside the tank. With one opening at the top it ran the entire height of the tank down to about 35 cm above the bubbler. Here the tube made a 90 degree turn towards the centre of the tank and stretched to just outside the bubble plume where it had its other opening. The tube was used to inject a puff of fluorescent dye into the bubble plume. The dye was prepared by making a high concentration sodium fluoresceine solution in filtered seawater giving it the same density as the water in the experiment tank. The dye was injected with a syringe into the top opening of the tube,

approximately 5 ml at the time, and then water was injected behind it to push the dye to the lower opening and into the bubble plume in puffs of 1 ml.

The movement of the dye upwards through the tank was recorded with two systems simultaneously. The advancement to 30, 60, 90 and 120 cm was followed visually and the time measured with a stopwatch. A video camera was also set up beside the tank recording the movement of the dye for the first half metre. The additional monitoring system of the camera could then be used to calibrate the visual observation measurements. The experiment was executed three times in a row using the same water. After the third run the water was changed since it was too green to accurately follow the new dye that was injected. The experiment was performed during two different time periods (Table 1: Exp III-IV) using porous plate bubbler media grade 0,2; 2; 100 and 0,2; 20;100 respectively. In February 2008 (Table 1: Exp III), the experiment was run at two different pressure levels for each bubbler and always with the water level at 280 cm. In April (Table 1: Exp IV) measurements were made at three different pressure levels each being done with the water level at 240 and 315 cm. Each measurement was repeated three times during both experiment periods.

The dye study was focused on determining how bubble-size and air mass flow ( $Q$ ) affects the upwelling flow,  $V_{up}$ , in the centre of the bubble plume. The bubble size distribution was altered by changing the plate on the bubbler and a series of images was recorded for each case for later analysis (see 2.3.2 bubble size analysis). The images were taken through a bubble focuser at a height of 210 cm from the tank floor (190 cm above bubbler). The purpose of the bubble focuser, as the name suggests, was to direct the bubbles into the focus area of the camera. This improved image quality by minimising the number of bubbles in front and behind the depth of field. When the rising bubbles hit the wedge shaped sides of the focuser they were pushed towards the centre of the tank. As the bubbles reached the vertical midsection of the focuser they were forced into a gap, about 4 cm wide. On each side of the gap the focuser was fitted with a small glass window at the same height as the camera.

The air volume flow and pressure were precisely controlled and monitored with the air supply system (2.1.4 Air supply). Conversion of the volume flow of air to amount of substance was made with help of the ideal gas law

$$PV=nRT$$

where  $P$  is the pressure (Pa), here hydrostatic + “bubble production” (= PG2 in figure 8) + atmospheric pressure,  $V$  is the volume ( $\text{m}^3$ ), here per time unit (volume flow) from rotameters,  $n$  is the amount of substance (moles), which per time unit is referred to as mass flow ( $Q$ ),  $R$  is the ideal gas constant ( $8,3145 \text{ Jmol}^{-1}\text{K}^{-1}$ ) and  $T$  is the absolute temperature (K).

## ***2.3 Data treatment***

### ***2.3.1 Image processing***

A total of 538 thousand images were taken during the experiments. The first thing to do with these was to go through and sort out the ones with useful information i.e. images containing copepods. This was done manually with help of the graphic viewing program IrfanView. The screening process eliminated approximately 80 percent of the material leaving just over 100 thousand images for potential further analysis. All image analysis from here on out was made in the image processing program ImageJ. After learning the basics of this software at UCSB, under supervision of Dr. Ira Leifer, the following routine for image analysis was created.

Firstly, the images for destined for analysis were converted to 8-bit gray scale, if they for some reason were not already. Inverted look-up table (LUT) was also applied to make the images easier to work with. The LUT is the light intensity value for a pixel. It ranges from 0 to 255 (for 8-bit) where 0 is black and 255 is white. Hence, inverting the LUT results in the opposite.

The next step was to enhance image quality with a few of the programs built in filters. If there were any undesired stationary objects in the images, i.e. bubbles attached to the glass of the tank, they were removed with the z-projection function. When you have a series of temporally successive images the z-projection can create an image of the average light intensity of each pixel throughout the series. This means that a moving object, such as a rising bubble, will have a very low impact on the light intensity of a certain area of the image because it is in a different spot in each frame. A stationary object on the other hand will affect the LUT-value of the same pixels in every image and will there for be visualised as clearly in the z-projection as in all the images through out the series. When taking photos with high intensity direct backlighting it is hard to get a perfectly homogenous background. If there are spatial irregularities in the light intensities of the background, they will also be shown in the z-projection. To eliminate the unwanted elements the “image calculator” was used to subtract



the z-projection from all the images in the series, the entire “stack” in ImageJ terms. Another way to smoothen an uneven background is to use “subtract background” which, without going into all the details, distinguishes between objects and background by differences in the steepness of their light intensity gradient. In other words it will remove a subtle intensity gradient in the background due to uneven backlighting, but leave the bubbles. When reducing background noise with the methods mentioned above one should be careful not to subtract too much. If more than the lowest value in the image is removed the new value for those pixels is set to zero. That means a loss of information in the image.

Further fine-tuning of the images was done with “adjust brightness and contrast”. After that the scale was doubled resulting in twice the number of pixels along each axis of the image. Using interpolation, this gives objects with curved edges, like say a small round bubbles, a more smooth and circular appearance. Finally, the two processing tools “smooth” and “sharpen” were applied in stated order. The “smooth” application reduces noise by blurring the image. This filter replaces each pixel with the average of its 3x3 neighbouring pixels. The “sharpen” filter then re-increases the contrast of the image by yet again replacing each pixel with a weighted average of its neighbours. This further reduces the noise level of the images.

### ***2.3.2 Bubble size analysis***

Analysis of bubble size distribution was done with ImageJ’s built-in function “analyse particles”. This function measures particles of a certain size and circularity range, defined by the user. A small bubble has a shape very close to a perfect sphere. Hence, it is visualised in an image as a particle with a circularity value close to one. If the bubble density is high, there is likely to be overlap between bubbles in the images. Two bubbles of high circularity will be visualised as one particle with low circularity. Setting the minimum accepted circularity high will result in the program discarding these bubbles from the measurements. If there are larger bubbles present their circularity are also likely to be quite low, meaning that they will be discarded as well. If this was the case a second run of the analysis was done, this time with a lower limit for circularity and the addition of a higher value for the minimum size limit, above the size of small circular bubbles. Hence, an image series containing small and large bubbles were analysed twice, once for small circular bubbles and then again for larger ones with lower circularity.

Before running the particle analysis application the edges of the particle have to be defined. This was done with “adjust threshold”. This function tells the program what LUT-value gives the threshold for what is considered the edge of a particle. The particle edge in the image is not a perfectly sharp change from black to white but a gradient of the LUT-value. The gradient is the steepest for objects that are in focus and weakening with loss of focus. This means that when setting the threshold a small adjustment results in a very small change in the measured size of bubbles in focus but a rather large change in the size of non-focused bubbles. The best result is therefore attained if the bubbles out of focus are discarded before measuring. If the number of overlapped bubbles is too great to discard them all there is an option. If the centres of the overlapped bubbles are not too close together they can be separated with the “watershed” function. However, before applying this function the images must be converted to binary, eliminating all gray scale information. Then “fill holes” should be applied to prevent “watershed” from cutting up bubbles with bright centres into tiny fractions.

When a suitable threshold and circularity was found and applied the “analyse particles” function returned measurements of “major” and “minor”, among other things, of each and every bubble in the image series. Bubble sizes, as equal spherical radius ( $r$ ), were then calculated with

$$r = \frac{\sqrt[3]{major^2 minor}}{2}$$

where *major* and *minor* are the largest and smallest values for the diameter of the best fit ellipse for the area of the particle .

Bubble size analysis was done on image series of 100-200 frames for quantitative measurement of bubble size distribution in plumes. The measured bubbles from an experiment case were divided into 25 or 50  $\mu\text{m}$  histogram bins and the number of bubbles from each bin transformed into bubble concentration in the plume centre,  $C_{bub}$  in bubbles/litre

$$C_{bub} = \frac{N_{bin}}{F * V_{meas}}$$

where  $N_{bin}$  is number of bubbles in each bin,  $F$  is number of frames in the image series and  $V_{meas}$  is the measurement volume. This, in turn, is given by

$$V_{meas} = D * (H - 2r_{bin}) * (W - 2r_{bin})$$

where  $D$  is depth of field,  $H$  is image height,  $W$  image width and  $r_{bin}$  is the mean bubbles radius in that bin. The bubble radius is subtracted from the image dimensions because bubbles touching the edge of the image are discarded in the size analysis process, meaning that the effective  $V_{meas}$  is smaller for larger bubbles.

Size analysis of bubbles attached to copepods had to be done manually. There are too many factors complicating an automation of this process. First and foremost discriminating between bubbles in front or behind, overlapping with the image of the animal and bubbles actually attached to it. This was done by following the bubble in question for several image frames. The great overlap between bubble and copepod also prevented the program from distinguishing the bubble as a separate particle. Thus, measurements were done manually with the line drawing tool in ImageJ, the only drawing tool not restricted to quantum steps of entire pixels. Hence, drawing a line across the bubble in question gave a good measurement of its diameter. If a bubble was large enough to show ellipsoid tendencies, the diameter was measured both vertically and horizontally. The values were then treated in the same fashion as for the major and minor described above. All size data were then converted from pixels to metric values with help of the calibration images taken for each experiment set-up (see “camera adjustment”).

### ***2.3.3 Computer software and Statistics***

The camera was controlled, and images stored with a custom made program designed in the computer software LabView. Initial sorting and filtering of images was done with IrfanView. For all other image processing ImageJ was used. Once the graphic data of the images was transformed into numeric data Microsoft Excel 2003 was used for storing and organising. This program was also used for simple data analysis such as tables, scatter plots, histograms and other graphs. More intricate statistical analyses were done in SYSTAT 10.2.

Attachment in filtered water and with added algae was for differences in bubble size distribution and ratio, i.e. the portion of copepods with attached bubbles. Size distribution was analysed with ANOVA and attachment ratio with a non-parametric Chi-square test. Results from the stamina experiment was analysed for sex or development stage specific differences in jump activity. Group (female, male and CV) were tested two by two with a t-test. In addition, data from three succeeding experiment runs using the same individual copepods

were tested for change the jump activity over time. A non parametric Kruskal-Wallis was used for this. Before performing parametric tests, the distribution of the data was analysed. Raw and log transformed data were plotted against expected Gaussian distribution. The data with the closest fit were then used for the statistical test. The significance level for testing the  $H_0$ -hypothesis (=no difference between groups) in all cases mentioned above, was set to  $p < 0,05$  for discarding  $H_0$ .

### ***3 Results***

#### ***3.1 Observations from pilot study***

A pilot study were performed in June 2007 (Table 1: Exp I) to test new equipment and get a basis for further development of experiments. These are the results and notes from that study:

Day 1: The first copepods were added to the tank (1m height) by injecting them straight into the bubble plume with a Peleus pipette. At first the animals showed signs of disorientation and followed the bubble stream upwards, but as soon as they became lucid they fled the bubbles by actively jumping away. However, the first bubble attachment was observed (on the head, bubble diameter  $\approx \frac{1}{2}$  thorax diameter). During the next half hour the animals moved around the entire volume of the tank (no aggregation at bottom or surface) but kept out of the way of the bubble plume. After these observations it was clear that we need to force the copepods and bubbles to come in contact. Hence the installation of a vertical glass tube in the centre of the tank.

Day 2: With the new setup, glass tube in the centre of the tank, a few bubbles were observed on most animals. Smaller bubbles, 2-3 x antenna diameter, were often attached to the antennas, while larger ones ( $\frac{1}{2}$ -1\* thorax diameter) were attached along the body and at the end of tail and antennas. Some bubbles detached after just a few seconds while others stayed attached until the animal reached the surface. Here most bubbles detached or ruptured on contact with air. Some animals kept their vertical position in the bubble stream for a considerable time by active swimming, but when passive they were all brought up to the surface. Presumably this was more due to the upward water current driven by the bubbles than by flotation effect from the bubbles themselves. The observed number of attached bubbles was greater on dead individuals than living ones. The living individuals can probably shake off the bubbles or maybe the surface of the animals change as they die, e.g. from leaking substances that

enhance stickiness. In those cases when a larger bubble attached to the end of the tail or an antenna this part of the animal was turned upward, seemingly constraining the animals' ability to fight the upward pulling forces.

Day 3: When algal exudates were added to the tank observations of multiple bubble attachments per animal were more frequent. One individual was seen with at least 5 bubbles. Hence, there are positive indications on what can be expected when the experiment are started for real with all the equipment in place and working properly. However the observations so far are made on a small number of individuals, thus accompanied with a risk of bias.

### ***3.2 Attachment (big tank)***

In all, 604 copepods were examined for attached bubbles (Table 1: Exp II-III), from these 331 had attached bubbles. The size range of bubbles attached to copepods showed a near Gaussian distribution peaking at about 150  $\mu\text{m}$  radius, with a tail toward larger sizes (Figure 11A). The largest attached bubble was about 500  $\mu\text{m}$  and only three from a total of 643 attached bubbles larger than 400 $\mu\text{m}$ . The size distribution of attached bubbles does not strictly follow the distribution of the bubble plume (Figure 12). In all the experiments using porous plate bubbler the peak of attached bubbles was found at larger bubble size than the peak of size distribution in the plume. Even though, the maximum concentration of bubbles is found around 75  $\mu\text{m}$ , for all porous plate bubbles, quite few bubbles of this size were found attached. With the capillary tube bubbler, which had a bubble size peaking around 350  $\mu\text{m}$ , the most attached bubble size is shifted in the opposite direction, towards smaller bubble sizes (Figure 12). This indicates that the true optimal bubble size for attachment should be between 100 and 350  $\mu\text{m}$ . In this size range the attachment of bubbles follow the background distribution of the plume quite closely. Comparing the attached bubbles and bubbles in plume for bubblers P2 and capillary (Figure 12) it is clear that although there are high concentrations of 400-600  $\mu\text{m}$  bubbles, there are hardly any attachments in this size range. In all, 643 bubbles were found attached to copepods, this gives an average of 1,06 bubble per copepod in total or 1,94, excluding those with no bubbles. The distribution of bubble volume per copepod can be seen in Figure 11B. It is presented as the equal spherical radius for the combined air volume of attached bubbles on each copepod. The peak is found at 175 $\mu\text{m}$ , with the bulk or the test animals, 88 %, have attached bubbles equalling a radius of between 75 and 300  $\mu\text{m}$ .

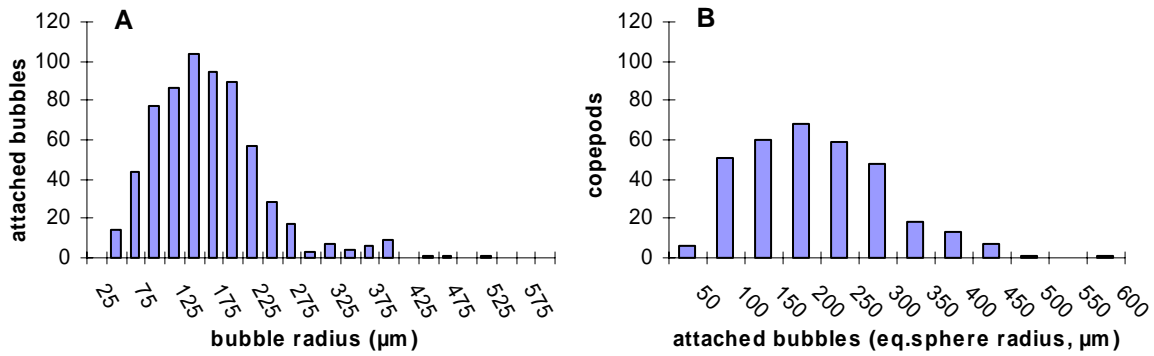


Figure 11. Size distribution of all bubbles attached to copepods in big tank attachment experiments showed a near Gaussian distribution with a tail toward larger bubble sizes (A). In all, 604 copepods were examined, from which 331 together had a total of 643 bubbles attached. The attachment level of copepods is given by the sum of all bubbles on each animal and presented as equal spherical radius for that air volume (B).

The attachment experiments in the big tank were done both in filtered sea water and with added algae. The addition of algae was meant to increase the stickiness of the water through the release of exudates, thus increasing the bubble-copepod attachment ratio. Statistic analysis (chi-square) of the attachment data shows no significant effect ( $p > 0,05$ ) comparing the two water qualities separately for each bubbler, table 2. The portion of copepods with attached bubbles is very similar in both cases. Over all 55 % of the examined copepods had bubbles attached to them, 49 and 53 % in filtered water and added algae respectively. With low levels of added algae the attachment percentage was 66, however here only the 0,2 bubbler was used. The 0,2-bubbler gave the highest attachment percentage of the ones tested, 73, 66 and 66 % for filtered, high and low algae concentrations. The bubbles that were attached to copepods in filtered water and with added algae were also tested for differences in size distribution using ANOVA. The size distributions for the two water quality groups can be seen in Appendix A. No significant difference was found,  $df=1$   $F\text{-ratio}=0,43$   $p=0,511$ . ANOVA was done on log transformed data, because these were shown to have a near Gaussian distribution (Appendix B). The data attained from experiments using capillary tube bubbler was not enough for significant statistical analysis. Over all very low attachment ratios were achieved with this bubbler, 24 % for all data combined (Table 2).

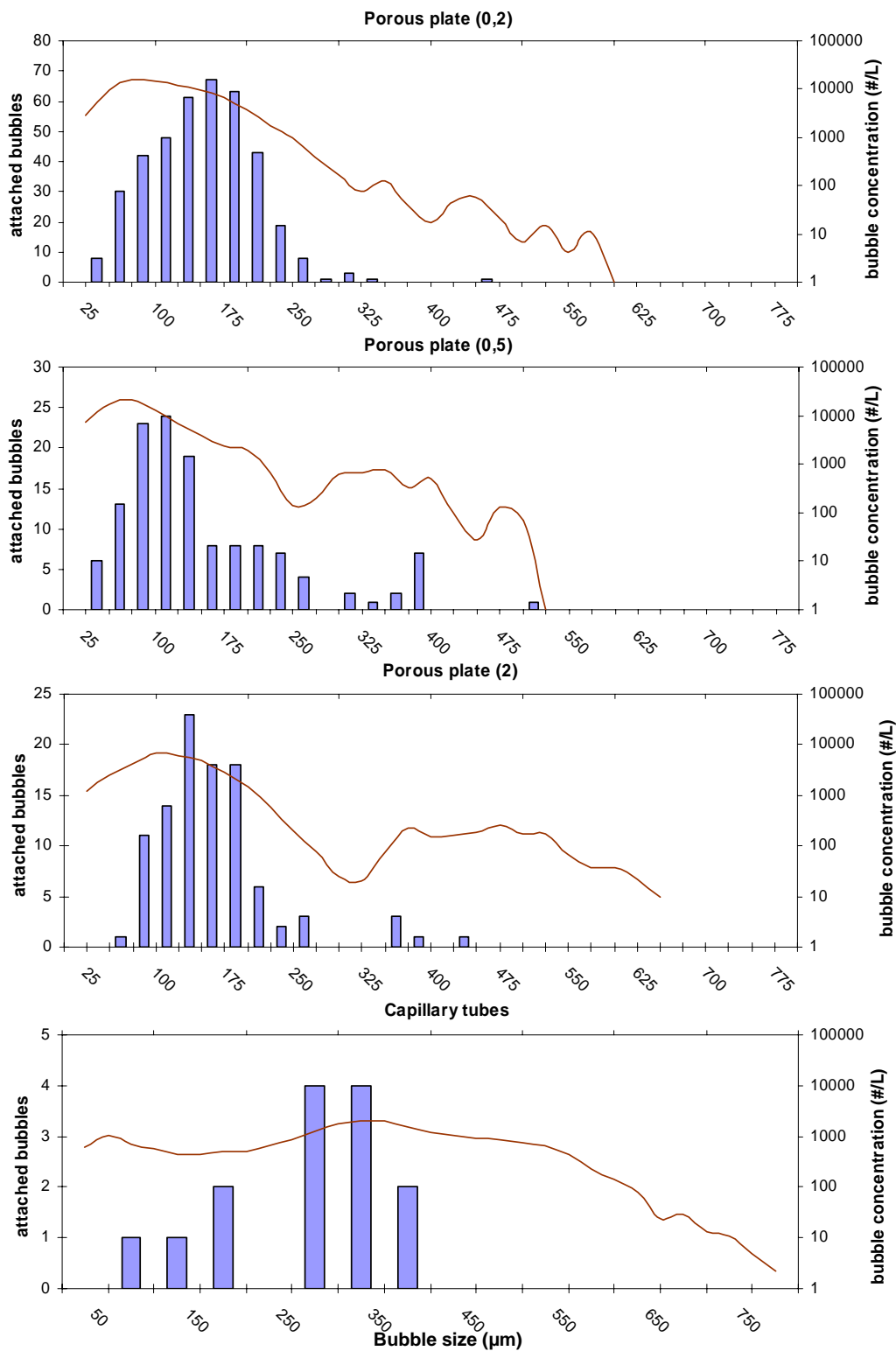


Figure 12. Size distribution of bubbles attached to copepods (bars) and the bubble size distribution in the plume generated by that bubbler (line, logarithmic y-axis).

Table 2. Attachment ratio shown as portion of copepods with attached bubbles (%), N=number of copepods studied, presented for all bubbles (incl. third treatment group of low algae concentrations) and for filtered seawater and added algae separately (excl. low algae concentration) for each bubbler. Chi-square test was done for difference between the two treatment groups, filtered and algae. No significant differences were found.

bubbler	all		filtered		algae		$\chi^2$ -test		
	N	w/ bubbles	N	w/ bubbles	N	w/ bubbles	value	df	p
all	604	55 %	178	49 %	272	53 %			
porous plate									
0,2	283	67 %	48	73 %	80	66 %	0,621	1	0,431
0,5	192	43 %	74	42 %	119	45 %	0,225	1	0,635
2	88	56 %	44	45 %	44	66 %	3,73	1	0,053
capillary tube	41	24 %	12	17 %	29	28 %	0,549	1	0,459

Lifting effect on *Calanus finmarchicus* from attached bubbles was investigated by plotting the rise velocity of the animals against their attached bubble size (Figure 13). The analysis is based on pooled data from experiments using porous bubbler, 0,2; 0,5 and 2, only including series of more than 20 valid data points each.

The rise velocity of the copepods does increase with the level of bubble attachment. However, as an effect of turbulence in the plume, there is a very large variation in rise velocity, which diffuses the results significantly. The effect of bubble driven upwelling flow is also very evident. The copepods lacking attached bubbles showed considerable rise velocities, average: 4,5 cm/s; standard deviation: 1,6. The best fitted curve to the relationship between copepod rise velocity and attached bubble size is that of a polynomial function of second order. The function for this curve gives, under the studied conditions, a rise velocity of 4,4 m/s for a copepod with no bubbles attached, 5,3 m/s with the equivalent of a 250 $\mu$ m bubble and 8,7 with a 500  $\mu$ m bubble. Excluding the copepods with no bubbles, there is a good linear fit to the data (Figure 13).



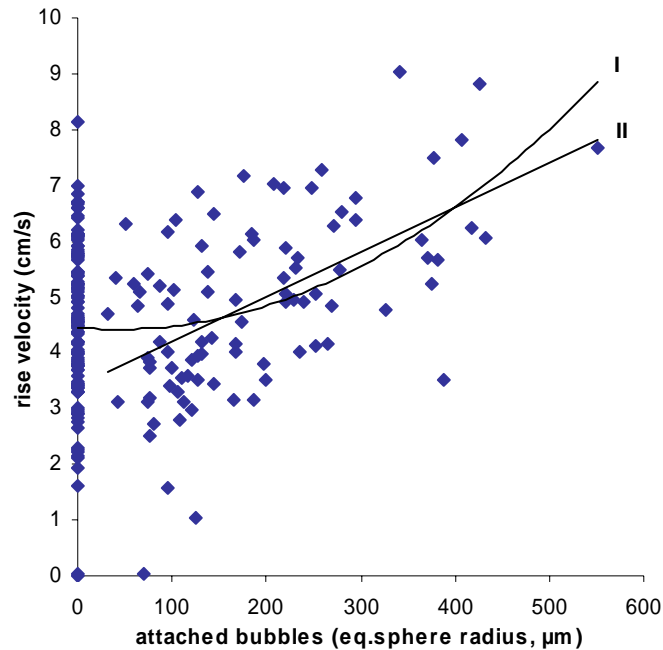


Figure 13. Relation between attached bubble size (sum of all bubbles on each animal presented as equal spherical radius for that air volume) and copepod rise velocity, trend lines are polynomial function of second order (I),  $R^2=0,1472$ , based on all data points, linear (II),  $R^2=0,3057$ , excluding copepods with no attachment. Total N=205; 93 with bubbles attached.

### ***3.3 copepod-bubble interactions (small tank)***

The small tank attachment experiments (Table 1: Exp III) show an attachment rate of 15 % (Table 3). That is, 15 % of the bubbles that collided with copepods attached successfully. Limited to collisions with bubbles in the size range of 175-400  $\mu\text{m}$ , the attachment rate is 20 %. In all, 54 copepod-bubble collisions were observed, 8 of which resulted in attachment. During the collisions where the bubble did not attach it either rolled along the body of the animal, following the curve of the body, or it bounced, changing its or the copepods direction abruptly at impact. The animals jumped away mainly when hit by bubbles larger than 350  $\mu\text{m}$ . In the few cases where jumps were induced by smaller bubbles the collision either took place on the antennas or by several bubbles at the same time. Jumping was also induced by bubbles passing without actually touching the copepod physically. This was observed for bubbles over 500  $\mu\text{m}$ . Examples of copepod-bubble interactions are visualised in Figure 14. See appendix C for details and notes.

### ***3.4 Stamina***

A stamina experiments was designed to test *C. finmarchicus* ability to avoid and eliminate attachment of bubbles. The test was done through stimulation with a glass rod, which induced

escape jumps by the copepods (Table 1: Exp II, V). There was a wide spread in the number of jumps performed by the copepods. Over all they kept reacting for a much longer time than anticipated, on average 95 jumps for the duration of 2 minutes for the females. The most durable copepod kept jumping for 10 minutes, completing 450 jumps, at which point the experiment was stopped due to exhaustion of the experimenter rather than the subject. There was a clear difference between male and female response to the stimulus (Figure 15). The females were much more resilient and kept jumping for longer than the males ( $t=5,223$   $df=7,4$   $p=0,001$ ; separate variance t-test). There was also significant difference between CV and males ( $t=3,542$   $df=11,6$   $p=0,004$ ), while no difference was found between CV and females ( $t=-1,714$   $df=14$   $p=0,109$ ). Only one from seven males performed more than 25 jumps (50) while only 4 of 45 females jumped less than 25 times. The sex specific difference in response pattern can also be seen in the number of jumps per time unit (Figure 15). The females clearly jump more frequently than the males.

Table 3. Interactions between copepods and bubbles. A total of 58 interactions ( $N_I$ ) were studied, including 54 collisions ( $N_C$ ) and 4 bubbles passing by without touching. The response rates show the percentage of the total number of collisions (physical) or interactions (behavioural) that resulted in each response, value for “attach” in brackets for 175-400  $\mu\text{m}$  bubbles.

response	physical			behavioural	
	attach	bounce	roll	jump	antenna flick
<b>N ( <math>N_C=54</math>, <math>N_I=58</math>)</b>	8	15	31	22	1
<b>response rate</b>	15 % (20)	28 %	57 %	37 %	2 %

The stamina experiments where the same individuals were used three times in a row with a short resting period in between showed no indications of exhaustion. There was no difference in number of jumps for succeeding experiment runs, Kruskal-Wallis;  $p=0,766$ . It is also clear that there are individual, i.e. not random, differences in jump performance. Copepods that jumped few times during the first run kept performing poorly for the succeeding two repetitions. Similarly, strong jumpers exhibited a high number during all three repetitions (Appendix D).

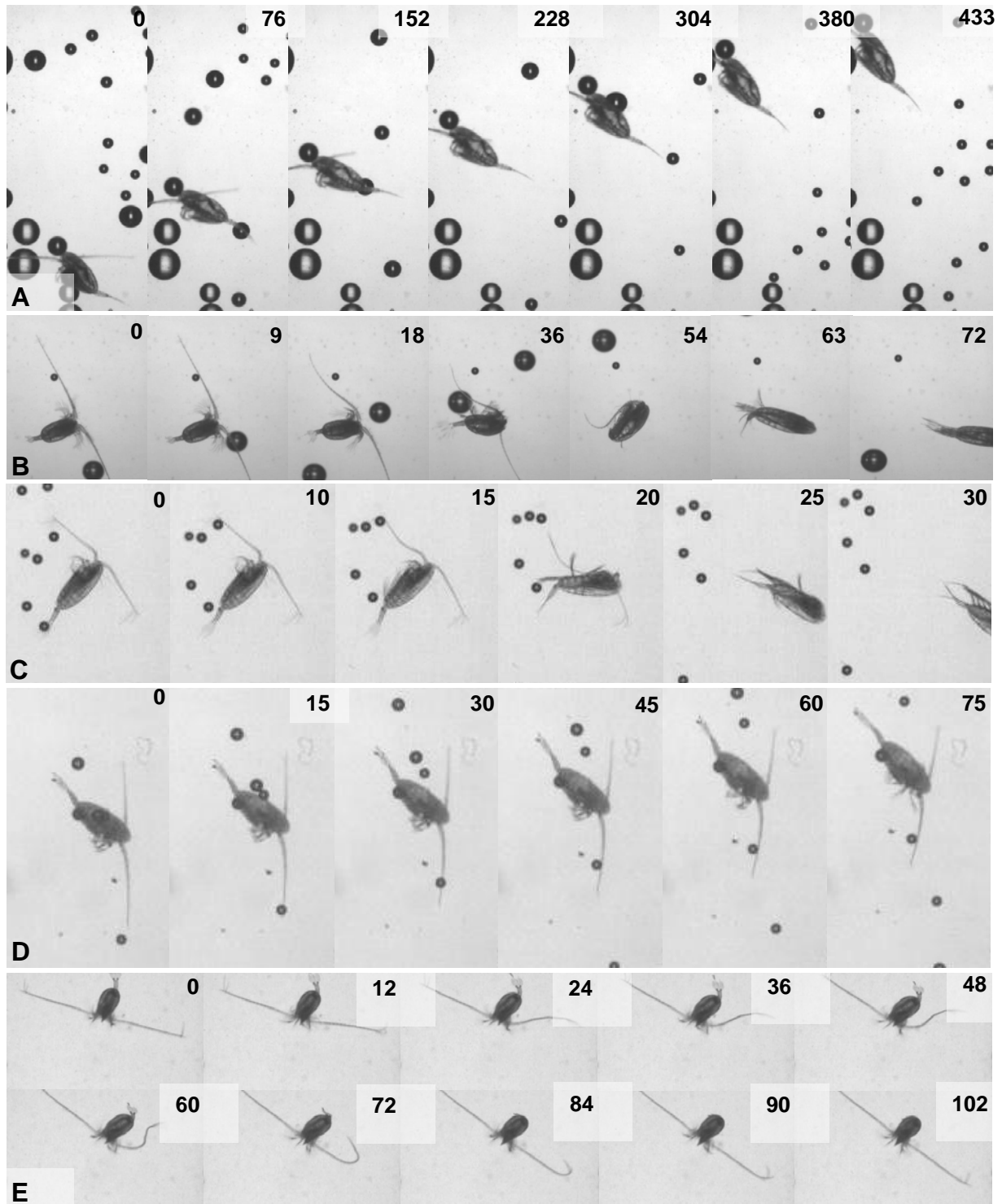


Figure 14. Timestamp in images is given in milliseconds. Examples of *C. finmarchicus*' response to bubbles: Bubble attached to head (A); animal swims one stroke (frame 2) which gives it a more horizontal position but the buoyancy force of the bubble turns the head back up and lifts the animal. Bubble attached to antenna (B) detaches when the animal performs an escape jump, possibly triggered by one of the bigger bubbles passing by. Bubble hits at tip of the antenna (C), triggering an escape jump. The copepod has one bubble attached ventrally close to the tail (D) and another one attaches to the antenna (frame 4). Flicking the antenna (E), a behaviour that has been observed several times as a response to bubbles attached to the antenna. Here it is performed for no apparent reason.

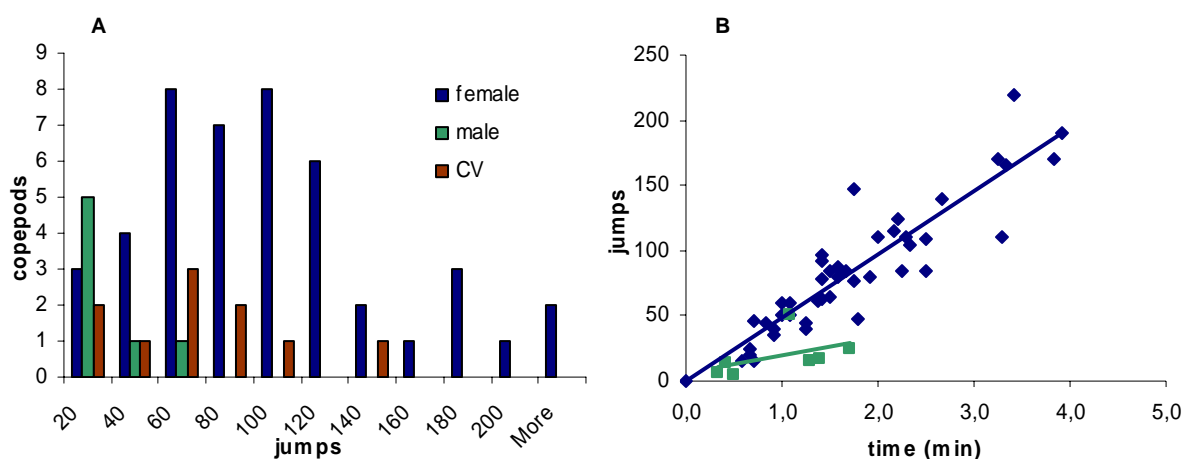


Figure 15. Number of escape jumps performed by copepods in response to repeated physical stimulus (A), total N=63 (45 female, 7 male and 11 copepodite V). Number of jumps plotted against duration of jump period (B) for adult males (green squares) and females (blue diamonds).

### 3.5 Bubble driven upwelling

The upwelling experiments (Table 1: Exp III-IV) produced flows ( $V_{up}$ ) of 5-35 cm/s. The highest flows were generated with the largest bubbles tested, produced with the P100-bubbler (Figure 16B). However, at low air flows the smaller bubbles produced higher  $V_{up}$  than the large ones per air mass flow ( $Q$ ). The relation between air flow and upwelling velocity was found to be  $V_{up} \sim Q^{0,23}$  for small bubbles and  $V_{up} \sim Q^{0,40}$  for large ones (Figure 16B). The flow measurements show the vertical transport of water in the centre of the plume. There is a vertical gradient in  $V_{up}$  in the centre of the plume, with lower velocities further away from the bubbler. The decrease is more or less linear for the first meter (Figure 16A). It was possible to follow the dye visually up to ca 120 cm above the bubbler. After this it became too diluted to follow the progression accurately. Velocity measurements were made with air flows up to 12,6 mol/h for the large bubbles. However, these higher flows resulted in a very turbulent upwelling pattern giving great variations in the rise velocity. Therefore these data were excluded from the analysis.

The bubble size analysis shows a comprehensive overlap in size distribution between the two finest bubblers while the coarsest one differs almost completely in distribution (Figure 17). Although, for some reason this bubbler produced different sized bubbles in the February and April experiments (Figure 17). The 20-bubbler produces a bimodal size distribution where the smaller bubbles are similar in size to the two bubblers of lower media grade and the larger

bubble fraction is partially overlapping the spectrum of the 100-bubbler. Because of its bimodal distribution the data from that bubbler was excluded from comparative analysis of the effect of bubble size on  $V_{up}$ . Since there is a great overlap in 0,2 and 2-bubbler distributions this data was pooled for this analysis. The same goes for the 100-bubbler data from the two experiment periods.

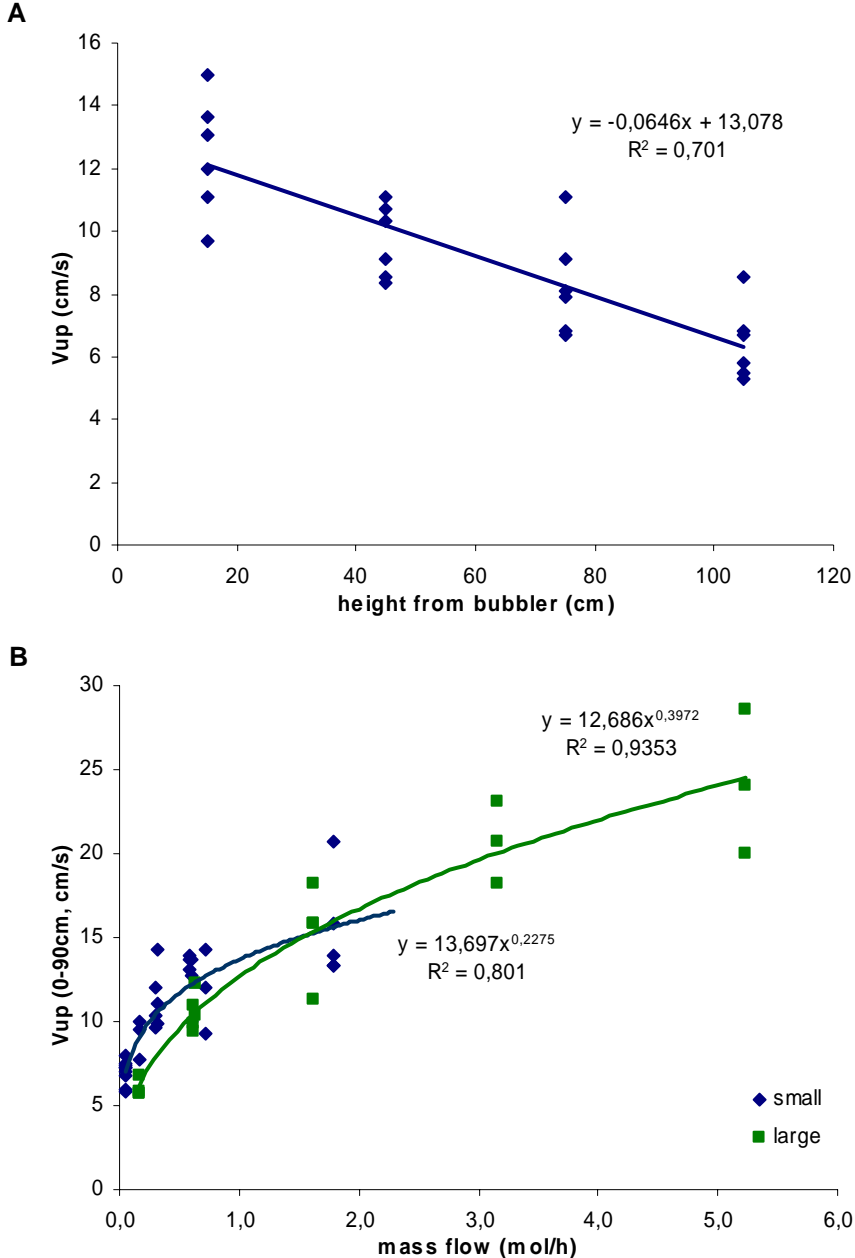


Figure 16. Change in upwelling velocity ( $V_{up}$ ) in centre of bubble plume with vertical distance from bubbler (A), for large bubbles (P100 in Figure 17) at  $Q=0,6$  mol/h.  $V_{up}$  is calculated average from 30 cm depth intervals and plotted at the middle depth within this interval. Relation between air mass flow ( $Q$ ) and upwelling flow ( $V_{up}$ ) for large (P100 in Figure 17) and small (P0,2+2 in Figure 17) bubbles (B). Velocities are average from bubbler to 90 cm above, lines showing best fit curve to data, linear in (A) and geometric in (B).

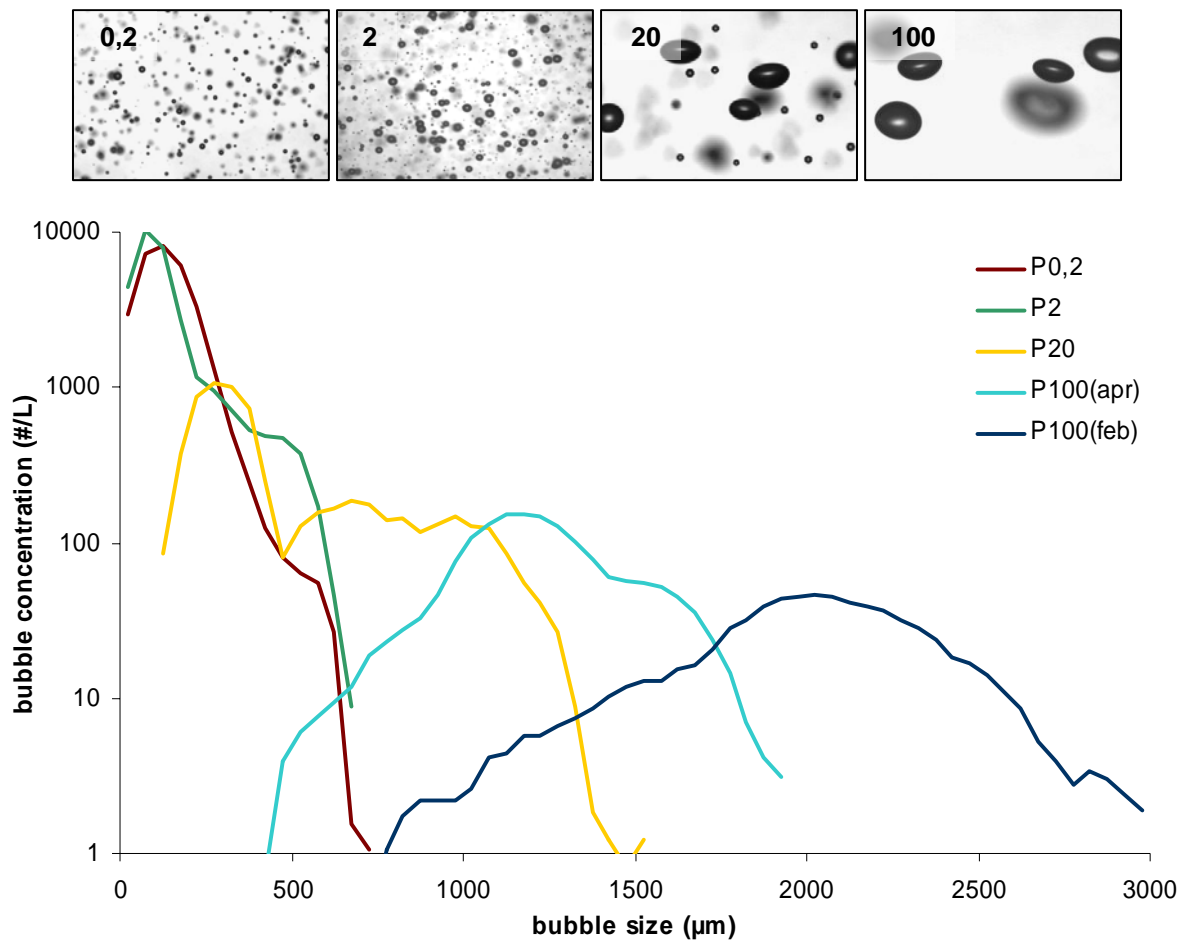


Figure 17. Bubble size distribution for bubblers used in dye upwelling study, series names indicate media grade of porous plates. Bubble sizes are visualised in images (upper panel) and size distribution curves (lower panel).

## 4 Discussion

Setting the upwelling properties of a bubble plume aside for now, what is the potential of flotation as a means to bring copepods from, say 20 meters depth up to the surface of the ocean? The maximum velocity, at which a particle can be lifted by a bubble, is the rise velocity of the given bubble. The bigger and heavier the particle is the further the actual rise velocity of the aggregate will be from that of the bubble itself. Under the given circumstances, the rise velocity of bubbles is mainly determined by their size (Patro et al. 2002). Rise velocities for bubbles in sea water are very close to those modelled for clean water (Figure 1). The most effective bubble size for attachment to *Calanus finmarchicus* in the current study was 125-225 µm. As the volume and thus buoyancy increases exponentially with radius the higher end of this size range is more important for flotation.

A 200  $\mu\text{m}$  bubble has a rise velocity of about 4 cm/s. A single bubble of this size contributes very little to the flotation of a copepod, since its air volume is very small. The rise velocity of a copepod with a 200  $\mu\text{m}$  bubble will therefore be substantially less than 4 cm/s. A lot of the copepods had more than one bubble each. The majority of the test animals had an attached air volume equal to that of a 50-300  $\mu\text{m}$  bubble. Still, a 300  $\mu\text{m}$  bubble can only give the animal a rise velocity lower than 6,6 cm/s, which is the rise velocity of the bubble. The largest bubble attached to a copepod in the current study was 5000  $\mu\text{m}$  in radius. A bubble of this size has a rise velocity of about 15 cm/s in clean water. From 20 meters depth, this gives it a theoretical time to reach the surface of just over two minutes (130 seconds) up to the surface. If the fishing boat towing the bubbler is moving at a speed of one knot, the last copepods will surface 70 m behind the bubbler. A distance that sounds quite manageable for a bigger boat in the open ocean. As the surfacing area is moved farther away from the boat, the more difficult it becomes to manoeuvre the trawl into the correct position (pers. obs.<sup>2</sup>). However, it is unlikely that the velocity of the copepod-bubble aggregate is very close to the rise velocity of the bubble it self. The results from this study on the attached bubbles' lifting effect show much lower velocities. The highest rise velocities recorded were around 9 cm/s. But only a small portion of the attained velocity is due to buoyancy of attached bubbles. Animals without bubbles also exhibited significant rise velocities and there was a substantial variation in the data. Hence, the attained rise velocities are largely explained by factors other than attachment of bubbles. The velocity of the copepods lacking bubbles is achieved mainly from bubble driven upwelling. The great variation in the data is likely due to the turbulent water flow in the plume, and also from differences in upwelling flow from different size bubbles. There is also a horizontally declining gradient in  $V_{\text{up}}$  radiating from the plume centre (Yum et al. 2008). Therefore, one can expect differences in rise velocity depending on the animal's horizontal position in the plume. To further limit the maximum lifting velocity provided by the attached bubble there is frictional drag which is created as the animal is being pulled through the water and the gravitational force acting on the slightly negatively buoyant copepod.

Finding a mathematical relationship for bubble attachment level and rise velocity of copepods is complicated due to the great variation in the data (Figure 13). The best fit is achieved with a linear function, excluding the data with no attachment,  $R^2 \approx 0,31$ ;  $N=93$ . The validation for

---

<sup>2</sup> Personal observation by author during field trials on board R/V Jan Mayen, June 2008

excluding the no attachment data is the possibility for a behaviour triggered by attached bubbles, affecting the lifting process. Copepods with no bubbles exhibited a higher rise velocity than the theoretical given by extrapolation if the linear function. It is possible that attachment generally stimulates the copepods to e.g. swim down, which makes them less influenced by the upwelling current. This behaviour was observed during the small tank interaction experiments (Figure 14A). However, it is more likely that the relation between attachment and rise velocity is of a more exponential nature. The rise velocity is expected to be proportional to the volume of air attached. The volume ( $v$ ) in turn is proportional to the cube of the radius ( $v \sim r^3$ ), which is the independent parameter here. Based on this argument the closest fit curve to the data including no attachment, is that of a polynomial function of second order,  $R^2 \approx 0,15$ ,  $N=205$  (Figure 13). According to this curve the contribution to copepod rise velocity from a 500  $\mu\text{m}$  bubble is approximately 4cm/s. In the previously mentioned example with the fishing boat, a rise velocity of 4 cm/s would result in a rise time of over 8 minutes (500 seconds) from 20 m to the surface. In this case the copepods would surface 270 m behind the bubbler. Finding this surfacing area will be hard on the open ocean. Also, a lot can happen to the animals on the way up with stratification and currents in the water. Hence, the area on the sea surface where they appear is likely to be much dispersed, complicating the actual harvest. The conclusion here is that if flotation should be relevant in bringing copepods to the surface during bubble based harvest, attachment efficiencies need to be much higher than what was generally achieved in this study.

The current study on copepod-bubble attachment is dependent on good image quality. For this reason it has been done with relatively low bubble concentrations. Increasing the air flow, and thus the bubble concentration in the plume, will certainly increase the amount of successful attachments. However, with the current set-up it would be impossible to record any useful data. There would be too much noise in the images for successful analysis. There are other methods for measuring bubble size. However, for this type of study with relatively large quantities of bubbles, photography is probably the best option. The accuracy of this method can be improved by calibrating the measurements to the laboratory standard (Vazquez et al. 2005), which is the inverted funnel method. In this method the bubbles are caught in, as the name suggests, an inverted funnel, and from there enters a capillary tube where the volume of the air is measured. A third method for measuring bubble size is through acoustics. This gives very accurate measurements of singularly emitted bubbles, as they produce a “pop” of size dependent frequency when they are released by the bubbler.



In the experiments the copepods moved vertically through 75 cm of the bubble plume before being examined for attached bubbles. If a bubble harvest system in the sea is being towed at 20 m depth there will be a 20 metre high plume which is wide enough to prevent any significant horizontal escape of copepods. It is plausible that the attachment will be more effective in a large plume like this where the animals are surrounded by bubbles for a longer time period. However, to predict how attachment will be affected by such an up-scaling of the system one needs to determine the detachment rate as well. For a larger system to result in higher amounts of attached bubbles the attachment rates must be higher than the detachment rates, i.e. the animals must attain bubbles faster than they are losing them.

It has been concluded in the current study that the main reason for detachment under laboratory conditions is motility of the copepods, i.e. escape jumping. Female *C. finmarchicus* proved to be quite resilient, on average jumping 95 times, during 2 minutes, before becoming passive. For the optimistic flotation example with a rise velocity of 15 m/s, previously mentioned, this means that the average *C. finmarchicus* can perform escape jumps for the entire duration of the flotation process. Hence, their jumping behaviour is likely to have a significant effect on the efficiency of the flotation and concentration of copepods at the surface, the process on which this harvest method relies. In addition, the turbulent flow in the bubble plume is likely to increase the jump activity of the copepod. This effect from turbulence on copepod behaviour has been shown for several related species (Saiz & Alcaraz 1992, Hwang et al 1994).

The males were significantly less active jumpers than the females. They became passive sooner, after an average of 19 jumps. Their jump period lasted on average one minute, meaning that they also performed less jumps per time unit than the females. The difference in response between male and female copepods was expected given their different swimming behaviour. The male *C. finmarchicus* exhibit a cruising swimming pattern while females use the hop-and-sink technique to move around (Altin, pers. comm.<sup>3</sup>). Hence, the docile males seem better candidates for flotation than the females. However, they are not found in the same abundance as the females and copepodite IV and V (Pasternak et al. 2001). CV, which together with CIV are the most interesting stages for harvest, showed activity patterns similar

---

<sup>3</sup> Personal communication: Dag Altin, NTNU, NO-7491 Trondheim

to the females. Studies on interactions between *C. finmarchicus* and bubbles reveal an attachment efficiency of 20 % for bubbles in the size range of 175-400  $\mu\text{m}$  (Table 3). For more precise assessment of the attachment rate more data is needed, but this gives a good indication of what we can expect.

Another factor that can enhance the attachment in the field is surfactants (Malysa et al. 2005), e.g. from algal exudates (Mopper et al. 1995, Zhou et al. 1998). Adding the diatom micro-algae *Skeletonema costatum* to the experiment tank did not reveal any such effect. Only one species of algae was tested and only at concentrations equal to low spring bloom levels, ca. 1000 cells/ml. The amounts of exudates also change with the state of the algal cells, and progression of the bloom (Passow et al. 1994). Also, the algae were cultivated in a medium containing EDTA, which prevents flocculation of the cells (Alldredge et al. 1993). This could mean that it has an effect on the stickiness of the exudates. Tests should be done with combinations of algae typical for a spring bloom in Norwegian waters. Ideally the study should be done in situ, but studying copepods at individual level in the ocean is complicated. A potential micro-alga for enhancing attachment found in great abundance in Norwegian waters is *Phaeocystis spp.* This haptophycean has a very gelatinous appearance and is known to exude large quantities of hydrocarbons (Passow & Alldredge 1995). However, in areas of intense *Phaeocystis* blooms copepods are often scarce. This phenomenon may be explained by the alga's toxicity as well as their inhibitory effect on copepod feeding (Hansen et al. 2003, Dutz et al. 2005). Harvesting copepods in areas of high phytoplankton production presents a dilemma. On the one hand it may increase the efficiency of a bubble based system by increasing stickiness and thus attachment and flotation. On the other hand, trawling with fine meshed plankton nets in water containing large amounts of phytoplankton causes problems with clogging. Clogging of the net openings reduces the filtration efficiency considerably (Gjøsund 2006).

Assuming that sufficient attachment for an efficient flotation process can be achieved in the ocean, there are several advantages in using a bubble harvest system instead of conventional plankton net trawls. The first and most obvious one is use of smaller trawls. Hypothetically, a bubble system which is 10 m wide and towed at 20 meters depth brings all the zooplankton in the bubbling volume up to the meter closest to the surface. As the bubble plume stretches towards the surface it will grow in width slightly (Leifer et al. submitted 2008), making the surfacing area of the plankton about 15 m wide. Assuming that the animals are retained at or

very close to the very surface of the water column a one meter tall opening in the trawl should be sufficient. This means that a trawl with a 15 m<sup>2</sup> opening combined with a bubbler could bring in the catch from the same filter volume as a 200 m<sup>2</sup> conventional plankton net trawl. Downsizing of the trawl results in less towing resistance, especially when it comes to the fine meshed nets for plankton (Gjøsund 2006). Not that using a 200 m<sup>2</sup> is an option. Today's trawls have an opening of about 40 m<sup>2</sup> (Angell, pers. comm.<sup>4</sup>). The point is the potential for significant reduction of fuel costs.

With the understanding we have today of the dynamics in the marine food web, we know that a precautionary approach is required for management of a novel marine resource. It is difficult to predict the ecological consequences of a large scale zooplankton harvest. *C. finmarchicus* is found in great abundance along the Norwegian coast, and has an estimated yearly production of 74 million tonnes in the Nordic Seas (Aksnes & Blindheim 1996). Still, an extensive outtake within a limited area can result in local complications. The two main concerns with a copepod fishery in Norwegian waters are: competition for food with the larvae and fingerlings of commercially important species, and by-catch of fish larvae and eggs from ditto. For the first issue I believe that precautionary approach and close monitoring is the answer. Concerning by-catch, a bubble flotation harvest may provide a solution. If the size range of bubbles attaching to copepods is significantly different from that of other animals in the water, it is possible to be selective in the harvest process. The target species is lifted up to the trawl while other animals are left in the deep. This effect was not investigated in the current study, but a good basis for comparison was produced. The optimal bubble size for attachment to *C. finmarchicus* was found to be in the 125-225 µm size range. Almost no bubbles larger than 400 µm and very few smaller than 75 µm were found attached to copepods. That is even though 75 µm bubbles were the ones produced at the highest concentrations with all the porous plate bubblers. In order to investigate the effect on by-catch from a bubble harvest system, the attachment experiments of this study can be implemented on other marine organisms. Their optimal attachment size can then be compared with the values attained here.

Jellyfish can be efficiently floated with air bubble (pers. obs.<sup>5</sup>). Bubbles are caught underneath the bell and the animal is lifted rapidly to the surface. If the jellyfish are floated more efficiently than copepods, this may provide a solution to the by-catch problem

---

<sup>4</sup> Personal communication: Snorre Angell, Calanus AS, NO-9272 Tromsø

<sup>5</sup> Personal observation by author during field trials on board R/V Jan Mayen, June 2008

concerning these organisms. With the jellyfish lifted to the very surface of the water and copepods stopping slightly deeper, the trawl can be towed below the layer of jellyfish, thus minimising the by-catch.

There are many factors apart from bubble concentration, affecting the collision and attachment efficiency. Many of these factors depend on bubble size. Higher rise velocities give larger bubbles higher collision efficiency, i.e. a greater difference in velocity between bubble and particle results in higher probability for collision (Phan et al. 2003). But the effect of velocity difference on attachment efficiency is a bit more complex than that. More force on impact helps break through the boundary layer, which is necessary for attachment (Nguyen et al. 1997). On the other hand it can decrease the contact time between bubble and particle, thus negatively affecting attachment (Sven-Nilsson 1934). Collision angle also plays an important role here (Nguyen et al 1997, Phan et al. 2003). The bigger area covered by larger bubbles as they rise through the water also enhances their collision efficiency. For an accurate determination of the optimal bubble size for attachment all these factors need to be considered. Or, they should at least be kept in mind when interpreting the attachment results.

Studies on the lifting effect of attached bubbles on *C. finmarchicus* revealed an average rise velocity of 4,5 cm/s for copepods lacking bubbles. This vertical transport is due to bubble driven upwelling. Even at the low air flows used during these experiments, the upwelling effect is more important than bubble attachment for lifting the test animals. Higher upwelling velocities can easily be created by increasing the air flow. In dye releasing experiments, upwelling velocities of up to 35 cm/s were measured, average  $V_{up}$  from bubbler to 30 cm above. As the dye progressed vertically it slowed down (Figure 16B). The decrease was close to linear for the first meter from the bubbler and up. This decrease was greater than anticipated. Field experiments by Leifer et al. (submitted 2008) show a much more gradual decline of  $V_{up}$  with depth. One likely explanation is the measurements being done in the centre of the plume rather than as an average for the entire plume. As the plume expands horizontally, there will be a change in the radial velocity gradient (Schladow 1992), which results in declining velocity in the plume centre, further away from the bubbler. The fact that the current study was done in a laboratory tank also provides an explanation to the deviations with published data. The wall effect is considerable in a tank if this size (2.1.1 Big tank), and is definitely affecting the circulation pattern and upwelling flow driven by the bubble plume. Exactly in what way is more difficult to answer.

The upwelling experiments also revealed an interesting relationship between bubble size and upwelling. At low air flows, below 1-1,5 mol/h, the smaller bubbles were more effective in creating upwelling, while at air flows over this value the larger bubbles were better. All though the data are conclusive, more measurements at high air flow with small bubbles are needed to positively verify the superiority of larger bubbles in the higher flow range (Figure 16B). The relationship between bubble size and upwelling flow is an interesting topic for further investigation. The dye-injection experiment described in this study provides a simple but solid method for comparative analysis. A few improvements are suggested for future studies: A video recorder with an overview of the entire measurement height of the tank will provide more accurate measurements. As the dye becomes diluted it is difficult to follow visually. Since the dye (sodium fluorescein) is fluorescent it can be accentuated with ultraviolet illumination, which will further increase the accuracy of the results.

Upwelling velocity ( $V_{up}$ ) showed a geometric increase with mass air flow ( $Q$ ), where  $V_{up} \sim Q^{0,23}$  for small bubbles and  $V_{up} \sim Q^{0,40}$  for large bubbles. The relation for small bubbles compares very well with that of Leifer et al.(submitted 2008), who also presents  $V_{up} \sim Q^{0,23}$ . For large bubbles the result is closer to the Lemckert & Imberger's (1993) calculations of Milgram (1982) data,  $V_{up} \sim Q^{0,33}$ . So, the highest flows were created with the larger bubbles. Much higher pressure is needed to create large volumes of small bubbles than larger ones. This is due to the higher resistance of the fine porous plate needed for making small bubbles. Hence, from the bubble sizes tested in this study it is more efficient to use larger bubbles in creating a strong bubble driven upwelling.

Effects of attachment versus upwelling on copepods suggest that upwelling is more effective in lifting the animals towards the surface. However, there are some disadvantages to relying on the upwelling process for a zooplankton harvest system. This method is based on lifting the actual water mass and through that the animals contained in the water, all the animals. Suddenly the potential for differentiation of wanted and unwanted organisms is diminished. Then there is the problem with detrainment and intrusion from the plume. Especially in stratified environments the heavier water being lifted will leave the plume horizontally as its negative buoyancy gets too considerable. Any animals being lifted with it will probably follow the same route. As for the copepods being floated by attached bubbles, they are more likely to continue vertically with the rising bubble stream.

Lifting the water instead of just the animals in it will result in yet another complication. When the lifted water volume reaches the surface it will not stay there, but continue out from the centre of the plume, through so called outwelling. Or, in a stratified environment the water will plunge from the surface down to the level of neutral buoyancy and then flow away from the plume through intrusion (Lemckert & Imberger 1993). The water that was originally at the surface will be pushed away by the volume being lifted. Instead of getting a concentration of zooplankton at the surface the upwelling will only create a circulation of the water mass. This effect is very likely to present new challenges to the harvesting process. A surface skimmer or shallow plankton trawl will no longer be as efficient in collecting the catch as with the flotation method. Maybe the answer lies in a combination of large and small bubbles. Larger bubbles will create the upwelling flow to increase upward motion enough for the zooplankton to surface within a reasonable time window. Smaller bubbles attach to the animals and help keep them in the plume by making them less susceptible to detrainment during their vertical transport as well as downdraft once they reach the surface.

## ***5 Conclusions***

The most efficient bubble size for attachment to *Calanus finmarchicus* is 125-225  $\mu\text{m}$ . When taking into account the buoyancy effect of larger bubbles, the optimal bubble size for *C. finmarchicus* flotation will be found in the higher end of this range. However, at the attachment rates achieved in the current laboratory experiments the lifting effect of the attached bubbles was low. Effects up bubble driven upwelling contribute more to the vertical transport of the copepods. However, there are several advantages to the flotation method compared to utilising upwelling in a bubble harvest system for zooplankton. First and foremost upwelling is likely to create circulation of the water mass and therein contained animals instead of concentrating the animals to the surface, which can be expected from a flotation process. Secondly, there is the issue of by-catch. The potential for a differentiated harvest, where the target species is brought to the surface while other organisms are left in the deep, is larger for a flotation based system. For flotation to be used successfully in a zooplankton harvest system, much more efficient attachment must be achieved in the ocean than what was done in the test tank. In order to estimate what level of attachment to expect in the field the detachment rates of bubbles need to be determined. The most common cause for detachment of bubbles was found to be the behaviour of *C. finmarchicus*. These animals'

capability to perform escape jumps can severely decrease the efficiency of the flotation process. On average the copepods could continue active jumping for 2 minutes, completing 95 jumps before becoming passive.

### ***Acknowledgements***

This study was funded by the Norwegian Research Counsel (NRC) through the project: “Harvesting zooplankton by bubble flotation” (project number 178421/S40).

First, I would like to thank all the people involved and contributing to this research project, and for giving me the opportunity to be involved in such an exciting and innovative project. I have really enjoyed my time working with you all; in Tromsø, Trondheim and Santa Barbara: My supervisor Roger Larsen and Kurt Tande, NCFS, for guidance and support during the entire process of this project. At SINTEF Fisheries and Aquaculture: Svein Helge Gjørund, Vegar Johansen, Håvard Røsvik, Eduardo Grimaldo, Arnstein Johannesen, Morten Bondø, Stig Jansson, Torleiv Njaa and Marte Schei for helping me with all the practicalities for the experimental work in this study; design and construction of equipment as well as providing me with everything I've needed. Altin, NTNU, for supplying me with test animals and information on ditto. Ira Leifer, UCSB, for introducing me to the fascinating world of bubbles and teaching me the basics of digital image analysis, and of course for showing me all the highlight of the Santa Barbara area. Snorre Angell, Calanus AS, for sharing knowledge on today's copepod harvest. Trond Larsen for proof reading and sharing literature.

All the teachers involved in the marine biology program at Lund University, Sweden: Thank you for providing me with a solid scientific education, before I left you for Norway.

Irene Whitney, Michael Ando, Tanya Danel and Emily Rancer: Thank you for hosting me during my stay in Santa Barbara. I really enjoyed your company and I am grateful for your support.

And last but certainly not least: Martina Jönsson for patience and understanding during my many months away from home throughout the work with this project, and for leaving your beloved home, Skåne, to join me in the far north. And also to my family for all the inspiration and support that helped me choose the path of science.

## References

- Aksnes, D.L., Blindheim, J., 1996. Circulation patterns in the North Atlantic and possible impact on population dynamics of *Calanus finmarchicus*. *Ophelia*. 44, 7-28.
- Allredge A.L., Passow, U., Logan, B.E., 1993. The abundance and significance of a class of large, transparent organic particles in the ocean. *Deep-Sea Research I*. 40, 1131-1140.
- Asaeda, T., Imberger, J., 1993. Structure of bubble plumes in linearly stratified environments. *Journal of Fluid Mechanics*. 249, 35-57
- Astthorsson, O.S., Gislason, A. 2003. Seasonal variations in abundance, development and vertical distribution of *Calanus finmarchicus*, *C. hyperboreus* and *C. glacialis* in the East Icelandic Current. *Journal of Plankton Research*. 25, 843-854.
- Bel Fdhila, R., Duineveld, P.C., 1996. The effects of surfactant on the rise of a spherical bubble at high Reynolds and Peclet numbers. *Physics of Fluids*. 8, 310-321.
- Buskey, E.J., Hartline, D.K., 2003. High-speed video analysis of the escape responses of the copepod *Acartia tonsa* to shadows. *Biology Bulletin*. 204, 28-37.
- Chen, S., Timmons, M.B., Aneshansley, D.J., Bisogni, J.J., Jr., 1992. Bubble size distribution in a bubble column applied to aquaculture systems. *Aquaculture Engineering*. 11, 267-280.
- Chen, X., Chen, G., Yue, P.L., 2002. Novel electrode system for electroflotation of wastewater. *Environmental Science and Technology*. 36, 778-783.
- Dutz, J., Klein Breteler, W.C.M., Kramer, G., 2005. Inhibition of copepod feeding by exudates and transparent exopolymer particles (TEP) derived from a *Phaeocystis globosa* dominated phytoplankton community. *Harmful Algae*. 4, 929-940.
- Ellingsen, K., Risso, F. 2001 On the rise of an ellipsoidal bubble in water: oscillatory paths and liquid-induced velocity. *Journal of Fluid Mechanics*. 440, 235-268.
- Fraser, A.J., Sargent, J.R., Gamble, J.C., 1989. Lipid class and fatty acid composition of *Calanus finmarchicus* (Gunnerus), *Pseudocalanus* sp. and *Temora longicornis* Muller from a nutrient-enriched seawater enclosure. *Journal of Experimental Marine Biology and Ecology*. 130, 81-92.
- Gjøsund, S.H., 2006. Flow through nets and trawls of high solidity. Report SINTEF Fisheries and Aquaculture report no. SFH80 A063012, Jan. 2006
- Han, M.Y., Kim, M.K., Ahn, H.J., 2006. Effect of surface charge, micro-bubble size and particle size on removal efficiency of electro-flotation. *Water Science and Technology*. 53, 127-132.
- Hansen, E., Eilertsen, H.C., Ernsten, A., Genevière, A.-M., 2003. Anti-mitotic activity towards sea urchin embryos in extracts from marine haptophycean *Phaeocystis pouchetii* (Hariot) Lagerheim collected along the coast of northern Norway. *Toxicon*. 41, 803-812.
- Heinonen, K.B., Ward, J.E., Holohan, B.A., 2007. Production of transparent exopolymer particles (TEP) by benthic suspension feeders in coastal systems. *Journal of Experimental Biology and Ecology*. 341, 184-195.
- Hwang, J.-S., Costello, J.H., Strickler, J.R., 1994. Copepod grazing in turbulent flow: elevated behaviour and habituation of escape responses. *Journal of Plankton Research*. 16, 421-431.



- Kattner, G., Krause, M., 1987. Changes in lipids during the development of *Calanus finmarchicus* s.l. from Copepodid I to adult. *Marine Biology*. 96, 511-518.
- Kattner, G., Hirche, H.J., Krause, M., 1989. Spacial variability in lipid composition of calanoid copepods from Fram Strait, the Arctic. *Marine Biology*. 102, 437-480.
- Kawamura, T., Fujiwara, A., Takahashi, T., Kato, H., Matsumoto, Y., Kodama, Y., 2004. The effects of the bubble size on the bubble dispersion and skin friction reduction. Proceedings of the 5<sup>th</sup> Symposium on Smart Control of Turbulence, University of Tokyo, Tokyo, Japan. February 29-March 2 (2004)
- Kepkay, P.E., Johnson, B.D., 1989. Coagulation on bubbles allows microbial respiration of oceanic dissolved organic carbon. *Nature*. 338, 63-65
- Kim, J.Y., Park, S.H., Kim, S.H., Park, H., 2006. Laboratory-scale analysis of effect of plume spacing of air diffuser system on destratification efficiency. *Environmental Technology*. 27, 1145-1151.
- Lalli, C.M., Parson, T.R., 1997. *Biological oceanography, an introduction*, 2<sup>nd</sup> edition. Butterworth-Heinemann, Great Britain.
- Leifer, I., Luyendyk, B.P., Boles, J., Clark, J.F., 2006. Natural marine seepage blowout: contribution to atmospheric methane. *Global Biogeochemical Cycles*. 20, GB3008, doi:10.1029/2005GB002668.
- Leifer, I., Jeuthe, H., Gjørund, S.H., Johansen, V., submitted 2008. Engineered and natural marine seep, bubble-driven buoyancy flows. *Journal of Physical Oceanography*.
- Lemckert, C.J., Imberger, J.I., 1993. Energetic bubble plumes in arbitrary stratification. *Journal of Hydraulic Engineering*. 119, 680-703.
- Malysa, K., Krasowska, M., Krzan, M. 2005. Influence of surface active substances on bubble motion and collision with various interfaces. *Advances in Colloid and Interface Science*. 114-115, 205-225.
- Mann, K.H., Lazier J.R.N., 2006. *Dynamics of marine ecosystems*, 3<sup>rd</sup> edition. Blackwell publishing, Cornwall, Great Britain.
- Maxworthy, T., Gnann, C., Kürten, M., Durst, F. 1996. Experiments on the rise of air bubbles in clean viscous liquids. *Journal of Fluid Mechanics*. 321, 421-441.
- Manley. D.M.J.P., 1960. Change of size of air bubbles in water containing a small dissolved air content. *British Journal of Applied Physics*. 11, 38-42.
- Milgram, H.J., 1983. Mean flow in round bubble plumes. *Journal of Fluid Mechanics*. 133, 345-376.
- Mopper, K., Zhou, J., Sri Ramana, K., Passow, U., Dam, H.G., Drapeau, D.T., 1995. The role of surface-active carbohydrates in the flocculation of a diatom bloom in a mesocosm. *Deep-Sea Research*. 42, 47-73.
- Myers, V.B., Iverson, L.I., Harriss, R.C., 1975. The effect of salinity and dissolved organic matter on surface charge characteristics of some euryhaline phytoplankton. *Journal of experimental marine Biology and Ecology*. 17, 59-68.
- Nguyen, A.V., Schulze, H.J., Ralston, R., 1997. Elementary steps in particle-bubble attachment. *International Journal of Mineral Processing*. 51, 183-195.

- Nicol, S., Endo, Y., 1999. Krill fisheries: Development, management and ecosystem implications. *Aquatic Living Resources*. 12, 105-120.
- Olsen, R.E., Henderson, R.J., Sountama, J., Hemre, G.-I., Ringø, E., Melle, W., Tocher, D.R., 2004. Atlantic salmon, *Salmo salar*, utilizes wax ester-rich oil from *Calanus finmarchicus* effectively. *Aquaculture*. 240, 433-449.
- Palanchon, P., Klein, J., de Jong, N., 2003. Production of standardized air bubbles: Application to embolism studies. *Review of Scientific Instruments*. 174, 2558-2563.
- Passow, U., Alldredge A.L., Logan B.E., 1994. The role of particulate carbohydrate exudates in the flocculation of diatom blooms. *Deep-Sea Research I*. 41, 335-357.
- Passow, U., Alldredge A.L., 1995. A dye-binding assay for the spectrophotometric measurement of transparent exopolymer particles (TEP). *Limnology and Oceanography*. 40, 1365-1335.
- Pasternak, A., Arashkevich, E., Tande, K.S., Falkehaug, T., 2001. Seasonal changes in feeding, gonad development and lipid stores in *Calanus finmarchicus* and *C. hyperboreus* from Malangen, northern Norway. *Marine Biology*. 138, 1141-1152.
- Patro, R., Leifer, I., Bowyer P., 2002. Better bubble process modelling: Improved bubble hydrodynamics parameterization. *AGU Monograph*. 127, 315-320.
- Phan, C.M., Nguyen, A.V., Miller, J.D., Evans, G.M., Jameson, G.M., 2003. Investigations of bubble-particle interactions. *International Journal of Mineral Processing*. 72, 239-254.
- Saiz, E., Alcaraz, M., 1992. Free-swimming behaviour of *Acartia clausi* (Copepoda: Calanoida) under turbulent water movement. *Marine Ecology Progress Series*. 80, 229-236.
- Sato, K., Sato, T., 2001. A study on plume behaviour in stratified water. *Journal of Marine Science and Technology*. 6, 59-69.
- Shladow, S.G., 1992. Bubble plume dynamics in a stratified medium and the implications for water quality amelioration in lakes. *Water Resources research*. 28, 313-321.
- Schladow, S.G., 1993. Lake destratification by bubble-plume system: design methodology. *Journal of hydraulic Engineering*. 119, 350-368.
- Sven-Nilsson, I., 1934. Einfluss der Berührungszeit zwischen Mineral und Luftblase bei der Flotation (in German). *Kolloid-Zeitschrift*. 69, 230-232.
- Tande, K.S., 1982. Ecological Investigations on the zooplankton community of Balsfjorden, northern Norway: Generation cycles, and variations in body weight and body content of carbon and nitrogen related to overwintering and reproduction in the copepod *Calanus finmarchicus* (Gunnerus). *Journal of Marine Biology and Ecology*. 62, 129-142.
- Tande, K.S., 1991. *Calanus* in North Norwegian fjords and in the Barents Sea. *Polar Research*. 10, 389-407.
- Tomiyaama, A., Celata, G.P., Hosokawa, S., Yoshida, S., 2002. Terminal velocity of single bubbles in a surface tension force dominant regime. *International Journal of Multiphase Flow*. 28, 1497-1519.
- Vazquez, A., Sanchez, R.M., Salinas-Rodríguez, E., Soria, A., Manasseh, R., 2005. A look at three measurement techniques for bubble size determination. *Experimental Thermal and Fluid Science*. 30, 49-57.

de Vries, A.W.G., Biesheuvel, A., van Wijngaarden, L., 2002. Notes on the path and wake of a gas bubble rising in pure water. *International Journal of Multiphase Flow*. 28, 1823-1835.

Watters, G., 1996. By-catch of fishes captured by the krill fishing vessel Chiyo Maru no. 2 in statistical area 58 (January to March 1995). *CCAMLR Science*. 3, 111-123.

Wiborg, K.F., Bjørke, H., 1969. Undersøkelser av forekomst og prøvafiske av raudåte I fjorder og kystfarvann mellom Fedje og Boknfjorden i mai-juni 1969 (in Norwegian). *Fiskets Gang*. 55, 819-822.

Wiborg, K.F., Hansen, K., 1974. Fiske og utnyttelse av raudåte (*Calanus finmarchicus* Gunnerus) (in Norwegian). *Fisken og Havet. Serie B* (10), 1-25.

Wu, M., Gharib, M., 2002. Experimental studies on the shape and path of small air bubbles rising in clean water. *Physics of Fluids*. 14, L49-L52.

Yum, K., Kim, S.H., Park, H., 2008. Effects of plume spacing and flowrate on destratification efficiency of air diffusers. *Water Research*. 42, 3249-3262.

Zhou, J., Mopper, K., Passow, U., 1998. The role of surface-active carbohydrates in the formation of transparent exopolymer particles by bubble adsorption of seawater. *Limnology and Oceanography*. 43, 1860-1871.

### **Internet**

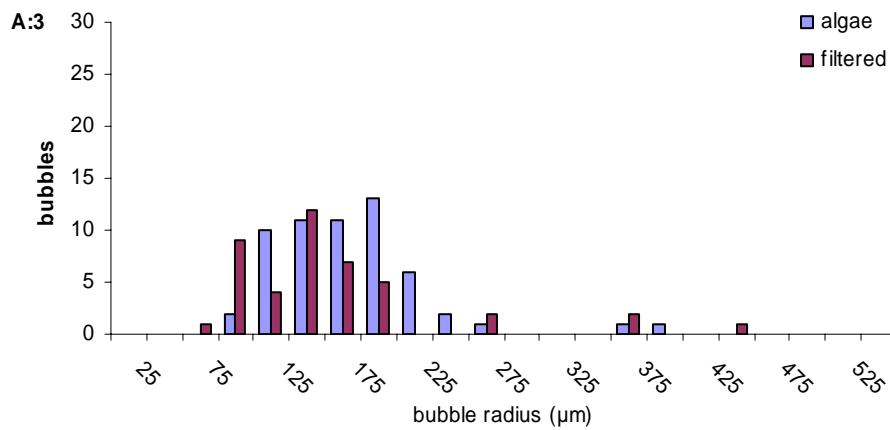
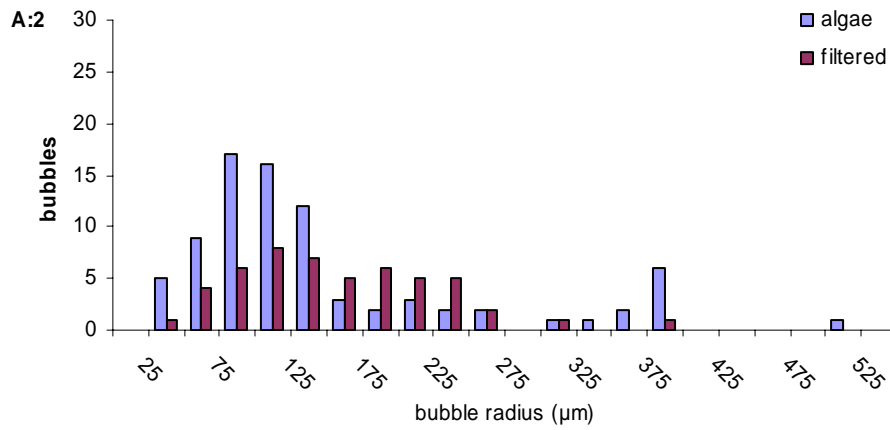
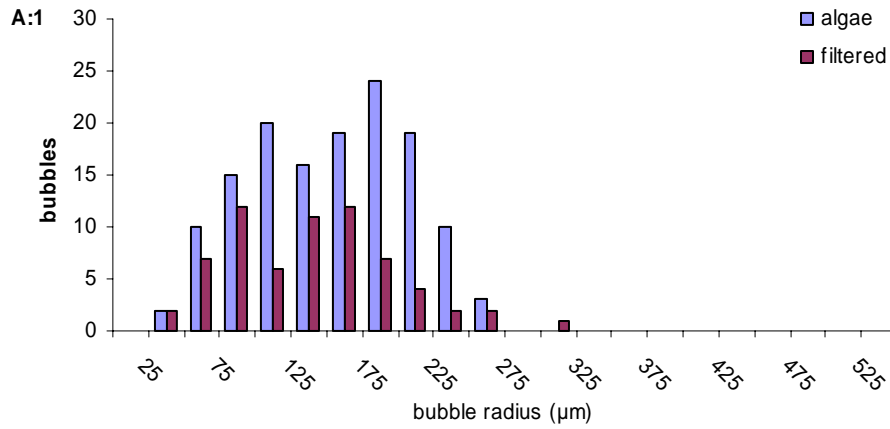
Electrochemistry encyclopedia, <http://electrochem.cwru.edu/ed/encycl/>. Bommaraju, T.V., Orosz, P.J., Sokol, E.A., 2001. Brine electrolysis.

Calanus AS, <http://www.calanus.no>

CCAMLR, <http://www.ccamlr.org>

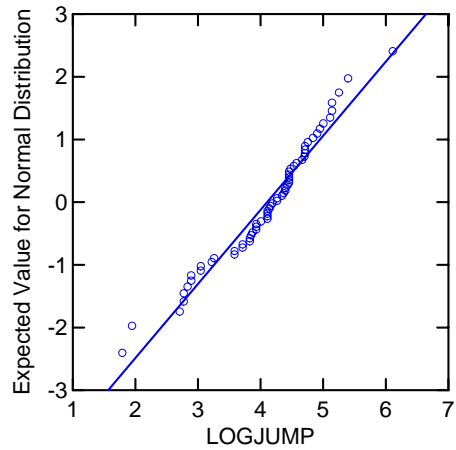
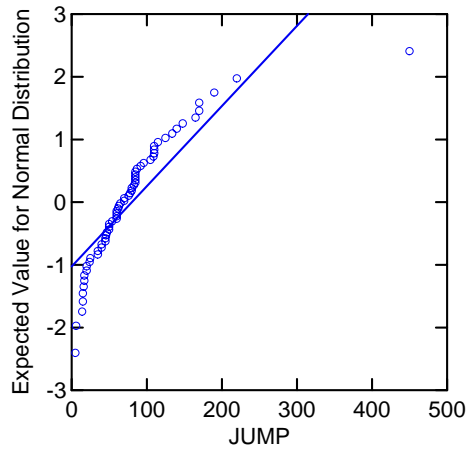
Hydrotechnik-luebeck, <http://www.hydrotechnik-luebeck.de> pages: Pneumatic Oil (Bubble) Barriers, Air in Water

**Appendix A. Attached bubble size in filtered and algae water.** Size distribution of bubbles attached to copepods in filtered seawater and with added algae, data presented for porous plate bubbler (media grade: A:1=0,2; A:2=0,5; A:3=2).

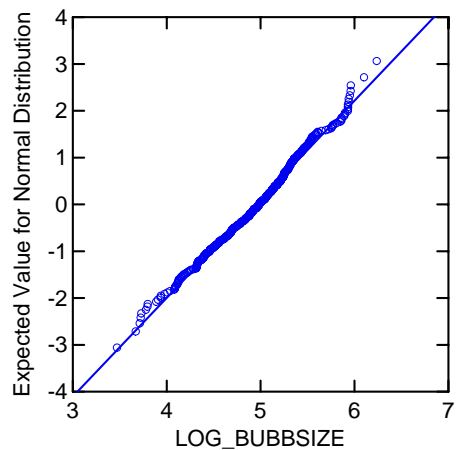
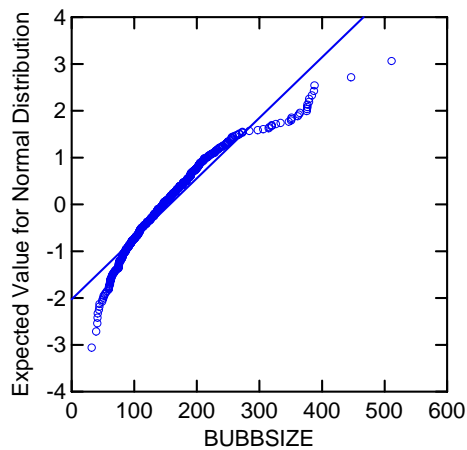


**Appendix B. Gaussian distribution test.** Probability plots to test Gaussian distribution of raw and log transformed data on number of jumps (B:1) in stamina experiments for testing sex or stage specific differences and size distribution (B:2) of bubbles attached to copepods in filtered seawater and with added algae. In both data sets the log transformed data is closer to Gaussian and therefore better suited for statistical variance analysis (A for t-test and B for ANOVA).

**B:1**



**B:2**



**Appendix C. Copepod-bubble interactions.** Data and noted observations from the small tank copepod-bubble interaction study.

<b>interaction</b>	<b>anatomic position</b>	<b>radius (<math>\mu\text{m}</math>)</b>	<b>notes</b>
attach	antenna	179	
attach	antenna	179	
attach	antenna	179	
attach	dorsal prosome	204	hits the back and rolls successively to head
attach	tail	179	
attach	tail	217	second bubble hits closer to tail end,
attach	ventral prosome	230	
attach	ventral prosome	357	caught by extended back periopods, detached after 70 frames by jump.
bounce	dorsal prosome	434	
bounce	dorsal prosome	421	
Flick+bounce	antenna	357	flicks when bubble hits near tip of antenna
Jump+bounce	dorsal prosome	485	pushed aside, uncertain jump
Jump+bounce	head	485	half hearted jump
Jump+bounce	ventral prosome	421	bubble stays stationary 2 frames, all momentum transferred to copepod
Jump+bounce	ventral prosome	434	
Jump+bounce	dorsal prosome	357	hit by 2 more same size, jumps when hit by third
Jump+bounce	antenna	204	touches tip of antenna, starts jump next frame
Jump+bounce	antenna	421	hits mid antenna, starts jump next frame
Jump+bounce	antenna	485	jumps next frame
Jump+bounce	antenna	357	hits antenna tip, jumps after 2 frames
Jump+bounce	head	714	pushed aside by actual bubble (deformed) jumps immediately (1 frame)
Jump+bounce	tail	204	two hit appr. at same time, possibly not reason for jump
Jump+bounce	tail	242	
Jump+no touch	-	536	passing by near ventral side, probably touching periopods
Jump+no touch	antenna	242	hardly touching tip of antenna, starts jump after 1 frame
Jump+no touch	dorsal prosome	663	no touch, only passing bow wave, jump after 2 frames
Jump+no touch	dorsal prosome	816	probably just bow wave, jump after 2 frames
Jump+roll	antenna	357	antenna tip
Jump+roll	dorsal prosome	1020	pushed aside by bow wave then jumps
Jump+roll	head	357	
Jump+roll	head/antenna	357	jumps next frame
Jump+roll	ventral prosome	357	near tail, jumps after 5 frames
roll	antenna	179	
roll	antenna	196	
roll	antenna	357	hits mid antenna, rolls in to body moves copepod slightly
roll	antenna	434	
roll	dorsal prosome	255	
roll	dorsal prosome	255	
roll	dorsal prosome	217	bubble pushed by copepod for 12 frames

<b>interaction</b>	<b>anatomic position</b>	<b>radius (µm)</b>	<b>notes</b>
roll	dorsal prosome	230	
roll	dorsal prosome	179	2 in a row, same parametres
roll	dorsal prosome	179	
roll	dorsal prosome	179	
roll	dorsal prosome	179	
roll	dorsal prosome	204	
roll	dorsal prosome	204	
roll	dorsal prosome	357	
roll	dorsal prosome	357	
roll	dorsal prosome	357	
roll	dorsal prosome	230	
roll	head	357	rolls over back
roll	tail	179	
roll	tail	217	
roll	ventral prosome	485	
roll	ventral prosome	472	
roll	ventral prosome	357	
roll	ventral prosome	230	
roll	ventral prosome	255	

**Appendix D. Repeated Stamina experiment.** The stamina experiment was repeated three times for five copepods in order to see if there was any change in jumping activity over time, e.g. due to exhaustion. Test subjects had approximately 20 minutes of rest between repetitions. According to statistical analysis (Kruskal-Wallis) there is no difference between repetitions,  $p=0,766$ . The results also show that there are some individual differences in performance, rather than being completely random.

Copepod \ Repetition	1	2	3
1	47	90	125
2	109	37	94
3	16	11	8
4	110	150	165
5	85	79	90